F-PM-1S INTERACTIONS OF IONIC MOVEMENT AND GATING PROCESSES IN IONIC CHANNELS OF EXCITABLE MEMBRANES. Bertil Hille, Physiology & Biophysics, University of Washington Medical School, Seattle, Washington 98195.

Na and K channels are voltage-sensitive, ion-selective pores in nerve and muscle membranes. Individual channels open and close stochastically on a time scale of 100 μsec - 10 msec and, when open, select and pass single permeant ions on a time scale of 200 nsec. Axonologists are now trying to describe the processes of voltage-sensitive gating and selective permeation in molecular terms. A channel is thought to be a macromolecule with several interconvertible conformations, one of which is an open pore. The conformation changes can be detected as internal charge movements. The transitions are driven by the applied electric field and by the electric field of dipoles and the surface double layer acting on the charged groups of the macromolecule. The open pore provides a polar transmembrane pathway for ions to hop over a sequence of energy barriers, pausing for various times at binding sites on the way. Ions encountering high internal energy barriers or strong binding sites can clog the pore and can also alter the local electric field and other channel properties. By stopping current flow, a stuck ion produces an effect equivalent to changing the channel to a closed conformation. In addition, the ion may actually promote or impede such conformation changes. These modulatory effects are seen in dramatic form when organic cations pass in and out of Na or K channels but are also present with small inorganic ions. Even channels in closed conformations retain part of the polar pore and are affected by ions in it. The interactions of ionic movement and gating heighten the challenge of designing clear experiments and realistic models to understand the function of ionic channels. (Supported by USPHS grant NS08174)

F-PM-2S INTERACTIONS BETWEEN INTRINSIC MEMBRANE PROTEIN AND ELECTRIC FIELD. Charles F. Stevens, Department of Physiology, Yale University School of Medicine, New Haven, Conn. 06510.

Intrinsic membrane proteins can be driven from one conformation to another by imposed electric fields. The study of this phenomenon is relevant to understanding physical mechanisms underlying the nerve impulse because the gating behavior described by the Hodgkin-Huxley equations presumably reflects just such field driven conformational changes. An analysis of the interaction of imposed electric fields and membrane proteins, using the techniques of nonequilibrium statistical mechanics, reveals that the rate at which a membrane protein makes the transition from one of its conformational states to another depends exponentially $m(V)V$, where V is the membrane potential and $m(V)$ is the normal component of a quantity called the "equivalent dipole moment change" of the protein. The quantity $m(V)$ contains all complications arising from protein-membrane interactions and non-constancy of the membrane field. The $m(V)$ may depend upon V; that is, the equivalent dipole in general shows polarization. The precise voltage dependence of $m(V)$ must be determined experimentally, but the Debye low field limit might be expected to hold. In the limit of dipole energies small compared to kT, $m(V)$ should be approximately $m_0 + m_1V$. Earlier studies with the acetylcholine activated gates at frog neuromuscular junction showed that m_0 is approximately 50 debyes and that m_1V is neglegable over the usual experimental voltage range. More recent studies with a different species of frog have found that the m_1V term can be appreciable at usual voltages. In at least two instances, then, $m(V)$ can be described by the Debye low field approximation.

F-PM-3S IONIC MOVEMENTS AND INTERACTIONS IN THE GRAMICIDIN A CHANNEL. G. Eisenman, J. Sandblom,* E. Neher*, Dept. of Physiol., U.C.L.A. Sch. Med., Los Angeles, Ca.; Univ. of Uppsala, Sweden; Max-Planck-Institute Biophys. Chem., Göttingen, GFR.

Electrical signs of binding and interaction in the movements of Tl^+, K^+, Na^+, Cs^+, and H^+ cations through gramicidin channels are discussed as prototypes for analogous phenomena seen in Na^+ and K^+ channels of nerve. In chloride solutions, all complexities observed for ionic permeation in the neutral gramicidin A channel can be understood as consequences of interactions between cations in a multiply occupied channel for which a specific model is proposed which extends the Hladky-Läuger model for gramicidin by adding a specific cation binding site at the mouth of the channel. The theory of this model (J. Sandblom, G. Eisenman, and E. Neher, J. Memb. Biol., in press) successfully interrelates, through a set of experimentally measurable parameters, the concentration dependences of channel conductance in different salts, the phenomena of inhibition and block exerted by one ion on another (and on itself), and the complicated dependence on ion concentration of the permeability ratios as measured by zero-current membrane potentials in ionic mixtures. Using this model, the measured parameters are interpreted in terms of shifts in levels of energy wells and barriers within the channel resulting from binding of cations to the outer sites, and it is shown how the coefficients of all concentration dependent terms can be related to an intrinsic Eyring energy profile and its shifts with binding of various ions. The salient effects of introducing charged groups into the channel will also be discussed, particularly in relation to a secondary binding of NO_3^- and Ac^- anions which we believe occurs in cation-occupied channels of the initially uncharged gramicidin A, as well as by the direct attachment of anionic groups at the channel mouth accomplished by Apell, Bamberg, Alpes and Lauger in an O-pyromellityl gramicidin A analog. (Supp. by NSF (GB 30835) and USPHS (NS 09931)).

F-PM-4S THE ROLE OF MOLECULAR MOTION IN MEMBRANE EXCITATION. P. Mueller, Department of Molecular Biology, Eastern Pennsylvania Psychiatric Institute, Phila., Penna. 19129

Several compounds derived from bacteria and fungi (EIM, alamethicin, monazomycin, DJ400) form molecular channels in lipid bilayers. These channels exhibit voltage dependent conductance changes conforming to the Hodgkin-Huxley scheme. Chemical and kinetic evidence indicates that the gating process involves the voltage dependent insertion of the channel forming molecules into the hydrocarbon region and their subsequent aggregation by lateral diffusion into an open channel. The mathematical description of this process accounts quantitatively for the observed conductance kinetics including inactivation as well as other kinetic features that lie outside the Hodgkin-Huxley domain but are also observed in nerve. For alamethicin the single channel conductance fluctuations are in agreement with this excitation model and a complete set of the individual molecular insertion and aggregation rate constants has been derived from a combined analysis of single channel statistics and multi channel voltage clamp kinetics in a lecithin bilayer. In this lipid most of the alamethicin exists as monomer, the dimer formation is rate limiting and there is a positive free energy difference of 4 Kcal/mol between dimers and monomers. The rate constants are dependent on the lipid viscosity, are apparently diffusion limited and consistent with the estimated monomer concentration and diffusion rates. The relevance of this gating mechanism to cellular excitation will be discussed.

F-PM-A1 FORCE GENERATION BY VASCULAR SMOOTH MUSCLE CELLS. S. P. Driska and R. A. Murphy, Dept. of Physiology, Univ. of Virginia School of Medicine, Charlottesville, Va. 22901

Smooth muscle strips from the pig carotid artery can develop somewhat more isometric force than skeletal muscle normalized to cellular cross-sectional area with only a fifth of the myosin content and potential number of cross-bridges (R.A. Murphy et al., J. Gen. Physiol. 64: 691-705, 1974). The high force generating capacity might be due to (i) the way force is transmitted between cells, (ii) the geometry of the myofilaments within the cell, or (iii) intrinsic differences in the cross-bridge cycle. We tested the first hypothesis that the high force generating capacity of the tissue is due to the parallel mechanical coupling of cells anatomically arranged in series. If this were true, force generation in a parallel-fibered strip of the media of the pig carotid artery with a constant cross-section would show a dependence on the number of cells in the tissue, i.e., the overall length of a strip at L_o, the optimum cellular length for force development. Equilibrated strips were subjected to an isometric force-length determination and set at L_o (10.94 ± 0.45 mm (SEM), N = 9) where the maximum force developed to K^+ stimulation, P_o = 2.29 ± 0.18 x 10^5 Newtons/m^2 of strip cross-section. Two clips were sequentially introduced between the fixed end of the tissue and the transducer with P_o determined. The active forces developed by these shorter segments (N = 9) were unchanged: (1) L_o = 7.94 mm, P_o = 102 ± 1% (SEM) of control; (2) L_o = 4.94 mm, P_o = 100 ± 2%. We conclude that (i) cells anatomically arranged in series are mechanically coupled in a series force transmitting structure, (ii) normalization of force to cross-sectional area of the cells in the strip yields valid estimates of cellular force generation, and (iii) the high force output of arterial smooth muscle with its low myosin content is due to the properties of the cellular contractile system. [Supported by NIH grant HL 14547]

F-PM-A2 CALCIUM BINDING TO ACTOMYOSIN FROM BOVINE AORTA. G.D. Ford, R.Z. Litten*, and R.J. Solaro, Department of Physiology, Medical College of Virginia, Richmond, Virginia 23298.

Although it is generally accepted that tension development by vascular smooth muscle is triggered by increases in cytoplasmic calcium, there is very little quantitative information available concerning the binding of activator calcium to the contractile apparatus. To obtain such information calcium binding to a calcium-sensitive actomyosin preparation from bovine aorta was measured utilizing a centrifugation technique. Calcium binding to this aortic actomyosin could be described by the assumption of two classes of binding sites, one class having an apparent affinity of 3.07×10^5 M^{-1} and population of 0.22 μmoles of binding sites/g protein and the other class having an apparent affinity of 7.77×10^2 M^{-1} and population of 20.22 μmoles of binding sites/g protein. Calcium activation of the aortic actomyosin ATPase correlated with calcium binding to the low-affinity sites. This is directly opposite the situation observed in similar preparations from striated muscle. To relate the calcium binding observed in the aortic actomyosin to the situation in the whole muscle, the myosin content of the whole muscle homogenate and the actomyosin preparation was estimated by densitometry of SDS-polyacrylamide gels of the two fractions. Then calcium binding in the whole muscle was computed from the relation:
Calcium Bound/g muscle = (myosin content/g muscle)/(myosin content/g actomyosin) x Calcium Bound/g actomyosin.
Such an analysis yielded the result that approximately 40 μmoles Ca^{2+} must be bound per Kg of aorta for maximal activation of the aortic actomyosin. This is less than 50% of the amount of calcium required for full activation of striated muscle.

F-PM-A3 IN VIVO STUDIES OF CONTRACTION WAVE PROPAGATION AND ITS ROLE IN SPERM AND EGG TRANSPORT IN THE OVIDUCTAL ISTHMUS OF RABBITS, S.A. Halbert, P. Verdugo, J.L. Boling* and R.J. Blandau*, Division of Bioengineering and Department of Biological Structure, University of Washington School of Medicine, Seattle, WA 98195.

The isthmic portion of the mammalian oviduct transports spermatozoa and ova in opposite directions and at dramatically different rates. It has been hypothesized that the smooth muscle of the oviductal wall may effect both ovum and sperm transport, yet no one has been able to provide consistent evidence substantiating such a complex, dual function. We studied muscular activity of the oviductal isthmus in rabbits by using both direct observation and chronic monitoring with implanted transducers to determine the characteristics of contraction wave propagation during the pre- and postovulatory periods, i.e., the time of sperm and egg transport, respectively. During the preovulatory period contraction waves propagate throughout the isthmus uniformly in the pro-ovarian direction, at a speed of about 3 mm/sec and wave frequency 0.3 Hz. At this time stained fluid introduced into the isthmic lumen is transported rapidly and efficiently away from the uterus and into the oviductal ampulla (where fertilization takes place). In the post ovulatory period contraction waves are propagated only locally and their direction is random, i.e. essentially non-propagated segmental activity. This activity is associated with a pendular motion of luminal fluid without net transport in either direction. The contractile activity observed in the preovulatory period would certainly facilitate rapid sperm transport up through the isthmus. The random directionality of contractions during the post ovulatory period would, conversely, inhibit isthmic transport and could thereby play a major role in controlling ovum transport to the uterus. (Supported by NIH Contract NO1-HD3-2788)

F-PM-A4 EVIDENCE FOR FOLDING FIBERS IN A NON-STRIATED MUSCLE. R.K. Abercrombie*, Y. Matsumoto, and R.M. Bagby*, Dept. of Zoology, University of Tenn., Knoxville, Tenn. 37916, and Dept. of Physiology, Emory University, Atlanta, Ga. 30322

The non-striated fibers of sipunculid probroscis retractor muscles exhibit an ordered birefringent banding pattern. To study this phenomenon, a posterior proboscis retractor muscle of Phascolopsis (=Golfingia) gouldi was isolated and placed horizontally in a lucite chamber, in which agar coated Ag-$AgCl_2$ electrodes were embedded transversely with respect to the muscle. Tension was recorded via a RCA 5734 transducer with a Beckman Type RB Dynograph. The chamber was designed so a precise area of the muscle could be examined at various lengths. Polarizing optics revealed a banding periodicity perpendicular to the long axis of the muscle. The pattern in the muscle, based on structural analysis, is consistent with the assumption that the fibers have a zig-zag folded configuration. The thick filaments (27.0 nm) of each segment are generally parallel to the longitudinal axis of that segment and appear to interdigitate and to be discontinuous at the fold angle (V. Ernst, Ph.D. Diss., 1970). Our scanning electron microscopy of glycerol-extracted rigor muscle lends additional evidence to support a folding fiber hypothesis. Muscles examined at rest and during isometric tetanic contraction at various lengths revealed a change in birefringent band width. Band width increases as the muscle is stretched. In the neighborhood of L_o, there seems to be a linear increase in birefringent band width with stretch. This is accompanied by a decrease in band width during isometric tetanic contraction at the respective lengths in this region. The results of this investigation reinforce the hypothesis that a folding mechanism is responsible for the great shortening capability of this muscle. (Supported by NIH Grant HL18077-02.)

F-PM-A5 ELECTRICAL CONTROL OF FLAGELLAR ACTIVITY: POTENTIALS INDUCED BY DIRECT CURRENT INJECTION, AND TEMPERATURE DEPENDENCE OF THE ELECTRICAL CONTROL OF BULL SPERMATOZOON FLAGELLA. Peter M. O'Day and Robert Rikmenspoel, Department of Biological Sciences, SUNY at Albany, Albany, New York 12222

The control of motility in bull spermatozoa has been investigated using direct current injection through glass microelectrodes. We have previously shown by this technique that the injection of negative current into spermatozoa results in a decrease in the flagellar beat frequency. With a second impaling microelectrode positioned about 5um from the current injection electrode the potential induced by an injected current of -1.0uA was measured to be approximately -30mv. The decrease of flagellar frequency during the injection of -1.0uA of direct current shows a time course that is temperature dependent. The characteristic times measured were 10.8 $\pm$ 1.4 sec at 19°C, 7.4$\pm$1.1 sec at 25.5°C, and 1.6 $\pm$ 0.3 sec at 37°C, and the Q_{10} for the effect was 2.7 $\pm$ 0.5. We have also measured the Q_{10} for the flagellar frequency after impalement but before current injection and found a value of 1.5 $\pm$ 0.5. The dissimilarity between these Q_{10} values indicates that the mechanisms involved in the current injection control and in the flagellar beating powered by external ATP are different.
Supported in part by NICHD through grant HD-8752.

F-PM-A6 CONTROL OF FLAGELLAR MOTILITY IN EUGLENA AND CHLAMYDOMONAS BY MECHANICAL MICROINJECTION OF EGTA, EDTA, Zn^{++}, AND Mn^{++}. Kathleen M. Nichols and Robert Rikmenspoel, Department of Biological Sciences, State University of New York, Albany, N.Y., 12222.

The mechanical microinjection of Mg^{++} into Euglena and Chlamydomonas impaled with a microelectrode causes an increase in or an initiation of flagellar motility. Ca^{++} microinjected into these cells causes a decrease in flagellar frequency (J. Cell Biol., 10, 16a, 1976). When a Euglena, in a medium containing ATP, is microinjected with $<7x10^{-14}$l of 0.02M EGTA, a Ca^{++} chelator, the flagellar frequency does not change. The same result is obtained in Chlamydomonas with the injection of $<4x10^{-14}$l of 0.02M EGTA. Greater volumes of microinjected EGTA cause the flagellar motility to decrease. This suggests that a decrease in the internal Ca^{++} concentration does not stimulate flagellar beating in Euglena or Chlamydomonas. The microinjection of EDTA, which binds Ca^{++} and Mg^{++}, causes a decrease in flagellar beating. $7.5x10^{-14}$l of 0.02M EDTA, which diffuses to 0.4mM in Euglena, and $3x10^{-14}$l, equivalent to 1.2mM in Chlamydomonas, causes flagellar arrest. The microinjection of 0.1M Zn^{++} into these cells decreases the flagellar frequency similarly to the decrease in frequency caused by the microinjection of Ca^{++} and EDTA. The microinjection of $7.5x10^{-14}$l of 0.2M Mn^{++}, 0.4mM in an impaled Euglena, causes an approximate 1.5 fold increase in flagellar motility. Chlamydomonas flagella which stop beating upon impalement in a Mg^{++} free medium, resume a flagellar frequency of approximately 10cps when injected with $2x10^{-14}$l of 0.2M Mn^{++}. Supported in part by NICHD grant HD-6445.

F-PM-A7 CALCIUM EFFECTS ON CILIARY MOTILITY OF MUSSEL GILL CELLS AND REACTIVATED CELL MODELS. Marika F. Walter* and Peter Satir, Dept. of Physiology-Anatomy, University of California, Berkeley, Ca. 94720

The behavior of metazoan cilia depends on cytoplasmic concentration of calcium ion. In mussel gill (Elliptio) epithelia, lateral (L) cilia are arrested when the ionophore A23187 and 12.5 mM Ca^{2+} are added together (Satir, P. 1975, Science 190, 586). We have developed a method to show that Ca^{2+} exerts its effects on the gill cells directly. In a solution containing (A) 10 mM Na-phosphate buffer in 20-50 mM KCl or (B) 20 mM NaCl, 20 mM KCl in Hepes pH 7.4, single motile cells rapidly exfoliate from the tissue. Three motile cell types: L, laterofrontal (LF), and Frontal (F) cells -- can be distinguished. 50-60% of the cells remain motile for several hrs at room temperature. When 10^{-5}M A23187 is added to the cell suspension, motility is unaffected. Addition of 12.5 mM $CaCl_2$ without ionophore slightly increases the % motility observed. When Ca^{2+} and A23187 are added together, motility drops to 11-14% of control, presumably because Ca^{2+} now enters the cell cytoplasm. Cell suspensions were treated for 5 min with 0.03% Triton X-100 and washed in 30 mM Hepes and 0.1 M KCl, pH 7.3. This treatment resulted in loss of membrane integrity and corresponding total loss of motility. Aliquots of Triton-treated cells were reactivated with a solution containing ATP and Mg^{2+}. Nearly the same motility could be obtained after reactivation compared to motility in normal buffer A. When reactivation experiments were repeated in the presence of variable Ca^{2+} concentrations, the three cell types showed similar behavior: Ca-concentrations in the range of 0 to 10^{-5}M had little effect upon % motility. Above 10^{-4}M, reactivation of L-cells or groups of L-cilia dropped considerably, whereas LF-cells and F-cells were somewhat less inhibited. We conclude that Ca^{2+} acts directly on the ciliary axoneme itself. This work was supported by USPHS HL13849.

F-PM-A8 EVIDENCE FOR A CYTOPLASMIC DYNEIN. M.M. Pratt* and R.E. Stephens, Dept. of Biology, Brandeis University, Waltham, Mass. 02154 and Marine Biological Laboratory, Woods Hole, Mass. 02543.

Dynein, the ATPase from cilia and flagella, exists in two electrophoretic forms: a closely-spaced doublet with molecular weights >350,000. Upon release from the 9+2 axoneme, the enzyme sediments at 14S. Weisenberg and Taylor (1968) isolated from sea urchin eggs a 13S ATPase having enzymatic properties in common with dynein, suggesting that it was a ciliary precursor. Stephens (1972) observed one electrophoretic species in unfertilized eggs, comigrating with the higher molecular weight dynein A and showing no synthesis after fertilization, and found that a second band, comigrating with the lower molecular weight dynein B, was absent in the unfertilized egg but was synthesized after fertilization, implying that both must be ciliary precursors. Neither were identified enzymatically, however. We have confirmed the Weisenberg-Taylor observation of a 14S ATPase, using sucrose gradient centrifugation of whole egg homogenates, and have identified it with dynein A by comigration with authentic dynein obtained from cilia. A similar protein found in dogfish brain microtubules polymerized in vitro, suggested as dynein by Burns and Pollard (1974), also comigrates with dynein A. Pulse-labeling during induced ciliary regeneration indicates that sea urchin embryos are capable of synthesizing both dynein species, but the relatively low specific activity of dynein A implies that a fairly large pool of it exists before and after natural ciliogenesis. The very existence of dynein A in unfertilized eggs and the ability of the embryo to synthesize additional dynein A during regeneration adds further strength to the argument that dynein may serve some other energy transducing function in the cell in addition to its eventual utilization as a ciliary enzyme. Supported by NIH Grants GM 20644 and 21040.

F-PM-A9 PHOSPHORYLATION OF PRE-FUSION MYOBLAST MYOSIN INCREASES ACTIN-ACTIVATION S.P.Scordilis and R.S.Adelstein, Sect. on Molec. Cardiology, NHLBI/NIH, Bethesda, Md. 20014

Pre-fusion rat myoblasts (Yaffe L-5) in culture contain both myosin and myosin light chain kinase (MLCK). This myosin is of the cytoplasmic type (i.e., the light chains are 20,000 and 15,000 daltons). The myoblast MLCK catalyzes the incorporation of up to one mole of phosphate into one mole of the 20,000 dalton light chain of myoblast myosin. This MLCK is of the cytoplasmic type, in that it does not require Ca^{2+} for activity, whereas the muscle type of MLCK does require Ca^{2+}. These two types of MLCKs were studied using isolated denatured light chains from myosins of human platelets (PLT), canine cardiac (CCM) and rabbit psoas (RSM) muscle. Using $MgAT^{32}P$, the rates of phosphate incorporation into the light chains catalyzed by the pre-fusion myoblast MLCK were PLT > CCM > RSM, whereas the rates catalyzed by the rabbit psoas MLCK were RSM > CCM > PLT. The same site on the PLT light chain is phosphorylated by both the cytoplasmic and muscle MLCKs. This is suggested by the inability of the cytoplasmic MLCK to phosphorylate PLT light chains which were already phosphorylated by the muscle MLCK, even though the cytoplasmic MLCK could phosphorylate PLT light chains not incubated with the muscle MLCK under identical conditions. Unphosphorylated pre-fusion myoblast myosin showed no actin-activation of the low salt (0.017 M KCl) myosin ATPase; the specific activity without actin was 0.018 ($\mu M\ P_i$/ mg myosin/ min at 37°C) and with actin 0.019. However, phosphorylated myoblast myosin showed a marked actin-activation; without actin 0.017 and with actin 0.166. No change in the myosin high salt (0.5 M KCl) ATPase was observed; K_2EDTA unphosphorylated 1.28 and phosphorylated 1.31; Ca^{2+} unphosphorylated 0.23 and phosphorylated 0.22.

(S.P.Scordilis is a Fellow of the Muscular Dystrophy Association of America.)

F-PM-A10 REGULATION OF PHYSARUM ACTIN POLYMERIZATION. M. R. Adelman, Department of Anatomy, Duke University Medical Center, Durham, N.C. 27710

Since actin is readily extracted from Physarum plasmodia and exists in crude extracts (CX) in a monomeric form which will only polymerize under appropriate conditions, plasmodial movements might in part be controlled via regulation of actin assembly. Therefore the requirements for polymerization of pure actin were compared with those for the actin in CX. Our actin purification has been improved by the inclusion in all buffers of 5mM PP_i since PP_i inhibits the proteolytic production of the actin fragment BP (MW ∿37,000). BP is involved in the Mg polymer of Hatano, et al since only actin preparations devoid of BP polymerize (in 100mM KCl) to the same extent w/wo 1mM $MgCl_2$. The polymerization in CX of actin (endogenous or exogenous) requires optimal levels of KCl (∿100mM), ATP (1-2mM), and $CaCl_2$ (>10^{-5} M). The polymerization rate of purified actin is optimal at 100 mM KCl and falls off sharply at higher or lower [KCl]; however polymerization at 100mM KCl proceeds equally well over broad ranges of ATP (0.1 to 5mM) and calcium (10^{-8} to 10^{-3} M). The requirement for ATP in actin assembly in CX may be explained by the finding that ATP is rapidly degraded. There is an initial, calcium-dependent, conversion of ATP to AMP (presumably by the pyrophosphohydrolase of Kawamura and Nagano) followed by a slower reaction in which AMP disappears and ADP appears. PP_i inhibits both reactions, the second somewhat more strongly, and this may explain its prevention of actin proteolysis. We are now studying the extent to which the adenosine nucleotide metabolizing enzymes and/or associated factors play a role in regulating actin assembly. The calcium effects demonstrated in CX could reflect an indirect regulation of the G⇌F equilibrium; this would lead to control of motility either because actin filaments are required to transmit force or because F-, but not G-, actin activates myosin ATPase. Supported by NIH #s 2-R01-GM-20141 and 5-S04-RR-6148.

F-PM-A11 INTERACTIONS OF RED BLOOD CELL ACTIN WITH MYOSIN, SPECTRIN, α-ACTININ AND TROPOMYOSIN.† J. Maimon,* and S. Puszkin, Department of Pathology, Mount Sinai School of Medicine of the City University of New York, New York, N.Y. 10029

Red blood cell (RBC) -actin and spectrin were purified from human erythrocyte ghosts, while myosin, α-actinin and tropomyosin were purified from striated muscle. RBC-actin stimulated myosin-Mg^{2+}-ATPase severalfold. ATPase was linear with time up to 10 minutes and optimal at 37°C. ATPase was halved at 25°C. Spectrin, at equimolecular concentration with RBC-actin, enhanced RBC-actin effect. RBC-actin polymerization was accelerated in the presence of spectrin, α-actinin had a dual effect on RBC-actin-myosin interaction. At low and high concentrations it inhibited while at concentrations equal to RBC-actin, it stimulated RBC-actin-myosin-ATPase. Tropomyosin was found to cancel both spectrin and α-actinin effects on RBC-actin. When tropomyosin was added with troponin, the RBC-actin-myosin-ATPase activity became Ca^{2+} sensitive. The contractile, regulatory and structural proteins from muscle and erythrocytes studied were found adsorbed by the surface of polystyrene Lytron particles with high affinity-binding values. Molecular bilayers were formed with these proteins which correlated with their interactions for ATPase activation. The data suggest that RBC-actin has receptor sites for the binding of a membrane protein (spectrin), an anchoring protein (α-actinin) and regulatory proteins (tropomyosin-troponin).
† Supported by Grants #NS 12467 of NIH, and #75-811 of the American Heart Association. S.P., Established Investigator of the American Heart Association.

F-PM-A12 RAPID ISOLATION OF SPECTRIN-ACTIN COMPLEXES FROM INTACT RED CELLS. F. H. Kirkpatrick, Dept. Radiation Biology and Biophysics, University of Rochester School of Medicine and Dentistry, Rochester, NY 14642.

Washed red cells are lysed in 20 volumes of a solution containing 160 nM NaCl - 20 mM Tris-HCl, pH 7.4, and 1% Triton X-100, and centrifuged at 40,000 xg for 15', or 30,000 xg for 20'. The resulting pellet, invisible after centrifugation, is resuspended in the same volume of Tris-NaCl (without Triton) and recentrifuged. The final clear gel consists almost entirely of spectrin, actin, and traces of hemoglobin. The first-step pellet can be resuspended as individual "ghosts", which appear on negative staining electron microscopy as featureless (non-filamentous) ghosts or fragments (c.f., Yu, et al, J. Supramol. Struct. 1:312, 1974). The second-step pellet is highly aggregated, but can be dissolved at low ionic strength to yield spectrin and actin. The pellet contains proteases and will digest itself within 48 hours at 4°C. Solutions containing isotonic saline, tris and 1% Tween 20, 40, 60 or 80 or Brij 35, will not lyse red cells. Triton X-114 produces pellets essentially similar to Triton X-100. Lower concentrations of Triton X-100 in isotonic saline (e.g., 0.1% at 1:5 cells:medium) will not lyse cells, and Band 3 is depleted in the ghosts prepared by conventional hypotonic hemolysis of cells so treated. This method produces yields of spectrin and actin (per cell) at least as great as those obtained by conventional procedures. Spectrin and actin can be obtained in quantities useful for biochemical analysis from as little as 1 ml of packed cells, in about 30 minutes. This rapid and efficient preparation method will make possible studies of spectrin-actin complexes in the many interesting cases in which only a few ml of blood are available.

ERDA Publication Number UR-3490-1022.

F-PM-A13 FACTORS DETERMINING THE DESTRUCTION OF ACTIN FILAMENTS BY OSMIUM TETROXIDE. P. Maupin-Szamier,* and T.D. Pollard, Anatomy Department, Harvard Medical School, Boston, MA. 02115.

The electron microscopy fixative osmium tetroxide destroys actin filaments and we have studied this reaction to develop methods to preserve cytoplasmic actin filaments during preparation for electron microscopy. Upon reaction with osmium tetroxide actin filaments are broken into progressively shorter fragments, so the time course of the reaction can be followed by viscometry. The rate of actin filament destruction depends on the osmium concentration, buffer type, buffer concentration, pH and temperature and requires the continued presence of osmium. Under optimum conditions (0.1 M phosphate buffer, pH 6.0, 0^{o}C, 4 mM osmium tetroxide), the viscosity of actin solutions is stable for over 30 minutes, while under less favorable conditions, like those frequently used for electron microscopy fixation (e.g. 50 mM cacodylate buffer, pH 7.3, 25^{o}C, 40 mM osmium tetroxide) the viscosity of actin solutions decays with first order kinetics with a half-time of less than 5 minutes. Cross-linking the actin molecules within the filaments with glutaraldehyde does not prevent filament destruction by osmium. The mechanism of the filament destruction is unknown; however, osmium tetroxide cleaves the actin molecule into discrete peptides and oxidizes the cysteine and methionine residues, either of which could result in depolymerization. Actin-tropomyosin filaments are more resistant to destruction by osmium, accounting for the ease of preservation of muscle thin filaments for electron microscopy. (Supported by NIH Research Grant GM-19654)

F-PM-A14 INVOLVEMENT OF MYOSIN PHOSPHORYLATION IN PLATELET SECRETION. J.L. Daniel, H. Holmsen* and R. Adelstein, Specialized Center for Thrombosis Research, Temple University, Philadelphia, PA 19140 and Department of Molecular Cardiology, NHLI, Bethesda, MD 20014

Human platelets contain a kinase which phosphorylates the 20,000 dalton light chain of isolated platelet myosin (MLC). This myosin has a greater actin-stimulated ATPase activity in the phosphorylated than in the unphosphorylated form. We have now demonstrated that this phosphorylation can occur in intact platelets. Washed platelets were incubated with ^{32}P-orthophosphate. Myosin was isolated from these platelets by extraction in 0.5M KCl, 20mM Tris-HCl (pH 7.5), 3% butanol followed by precipitation by dilution to 0.1M KCl at pH 6.4. The location of ^{32}P in MLC was established by electrophoresis on SDS polyacrylamide and pH 8.6 urea polyacrylamide gels as well as by chromatography on Sepharose 4B. Addition of thrombin [5 NIH U/ml at 37°C for 5 min] to the intact platelets produced a 5-20 fold increase in the labeling of platelet MLC. The time course of MLC phosphorylation in response to thrombin was studied concurrently with that of ADP + ATP and β-N-acetylglucosaminidase (β-N) secretion. Phosphorylation occurred well before β-N secretion and concomittant or slightly before A-N secretion. These results are suggestive of a role of participation of contractile mechanisms in platelet secretion. (Supported by NIH training grant HL 05976.)

F-PM-A15 PROPERTIES OF PLATELET MYOSIN LIGHT CHAIN PHOSPHATASE. B. Barylko*, M. A. Conti*, and R. S. Adelstein, Section on Molecular Cardiology, NHLBI/NIH, Bethesda, Md. 20014

Platelet myosin light chain phosphatase was isolated from human blood platelets by preparing an alcohol-ether powder (Cohen, I. and Cohen C., J. Molec. Biol. 68, 383-387, 1972). The dried residue was extracted with 1 M KCl, 10 mM Tris·HCl (pH7.5), 1 mM EDTA and 2.5 mM dithiothreitol (DTT) for 8 h at 4^{0}. The extract was fractionated with saturated ammonium sulfate in 10 mM EDTA and the precipitated 40-70% fraction was dissolved in 1 mM $NaHCO_3$ (pH7.5), 2.5 mM DTT and chromatographed on a Sepharose 4B column equilibrated with the same buffer. A single peak of phosphatase activity was eluted as determined by phosphate release from p-nitrophenyl phosphate (PNP). Incubation of the pooled phosphatase peak with purified ^{32}P-labeled platelet myosin resulted in release of P_i with a concomitant reduction in actin-activated myosin ATPase activity. There was no evidence for proteolysis of myosin as judged by SDS-polyacrylamide gel electrophoresis. Platelet myosin light chain phosphatase could also be partially purified by Sepharose 4B gel filtration of the low ionic strength precipitate or the 35-50% ammonium sulfate fraction of platelet actomyosin, in 0.5 M KCl, 15 mM Tris·HCl (pH7.5), 1 mM EDTA, 2.5 mM DTT. The phosphatase eluted together with platelet myosin light chain kinase but separated from the kinase on DEAE-cellulose chromatography. This step also resulted in separation of at least two phosphatase fractions: a) a fraction active only with PNP that failed to bind to DEAE at pH7.5; b) a fraction that released P_i from ^{32}P-labeled myosin light chains, suppressed actin-activated myosin ATPase activity, was inactive with PNP and was eluted with a KCl gradient. Recently Morgan et al. reported on a purified skeletal muscle myosin light chain phosphatase (Biochem J. 157, 687-697, 1976). (B. Barylko is on leave from the Nencki Inst. of Expt. Biol., Warsaw, Poland).

F-PM-A16 INITIATION OF FILAMENT BUNDLE FORMATION. K.T. Edds. Marine Biological Laboratory, Woods Hole, Massachusetts 02543.

The coelomic fluid of all sea urchins contains cells that can dramatically change their shape during the formation of a cellular clot. Moreover, this morphological transformation can be induced in Strongylocentrotus droebachiensis and serves as a model system for cellular morphogenesis. These shape changes are the result of the reorganization of actin-containing filaments from a state of loose, apparently random, organization to one in which compact bundles of filaments are formed and radially arranged in the cytoplasm. The formation of the filament bundles is initiated at specific focal points on the cell's periphery and progresses inward. The initial stages of formation include the aggregation of several filaments at points perpendicular to the edge of the cell followed by the continued lateral aggregation toward the cell's center as the bundle increases in length. The filaments are thus realigned as they are gathered into the bundles that ultimately form the axial support for long, thin cytoplasmic projections (filopodia). A stellate shaped cell is formed as the membranous surfaces of the cell retract in between each filament bundle. The filopodial form is involved in a subsequent contractile event (clot retraction). The transformation appears to be necessary for the mobilization and arrangement of the contractile apparatus (filament bundles) and subsequent clot retraction.

Supported by Muscular Dystrophy Assoc. of America, Inc. and GM-23351 from the NIH.

F-PM-B1 WATER - CHROMATIN INTERACTIONS IN HELA CELLS AND THEIR KARYOPLASTS. P.T. Beall, P.N. Rao*, and C.F. Hazlewood. Baylor College of Medicine, Dept. Pediatrics and Dept. of Dev. Ther., M.D. Anderson Hospital and Tumor Institute, Houston, Tx 77030.

Previously (Science 192:904-907, 1976), we demonstrated a reproducible phase specific pattern of changes in the physical state of water during the HeLa cell cycle. Maximal freedom of motion of water molecules, as determined by nuclear magnetic resonance (NMR) spectroscopy is found in mitosis with spin-lattice relaxation time, T_1, for water protons of 1020 ms as compared to pure water at 3000 ms. Minimal freedom is found in S phase (T = 534 ms) where chromatin is diffuse. S phase cells treated with spermine, a polyamine with chromatin condensing activity, show an elevation of T_1 to 701 ms with no change in percent water content. Since chromatin is a major constituent of the cell, we tested the effect of conformational changes of chromatin on water in isolated nuclei. Karyoplasts from S and G_2 were obtained by the cytochalasin B enucleation method. Pelleted karyoplasts were subjected to a 180°-τ- 90° pulse sequence in a Bruker SXP NMR spectrometer at 30 MHz and 25°C for T_1 determinations. Whole S and G_2 phase cells had T_1s of 534 ms and 690 ms, while the karyoplasts were 457 ms and 692 ms, respectively. The lower T_1 of S karyoplasts suggests that water in the nucleus at this stage is more "ordered" than in cytoplasm. Incubation of S karyoplasts with spermine elevated T_1 to 617 ms with no change in percent water content. These data suggest that in HeLa cell cycle, the conformational state of nuclear macromolecules has a major influence on the T_1 values for cell water. This study confirms the dynamic relationship of water and macromolecules in living systems. This research was supported by the Robert Welch Foundation, the Office of Naval Research contract #N0014-75-A-0017, and NIH grant and contract GM-20154, and N01-CB-43978.

F-PM-B2 LOCATION AND CHARACTERISTICS OF THE CYCLIC NUCLEOTIDE PHOSPHODIESTERASE AND ADENYLATE CYCLASE IN EUGLENA GRACILIS. F. D. Schwelitz, S. A. Garges‡ M. E. Westgate‡ and H. D. Goldstein‡ Department of Biology, University of Dayton, Dayton, Ohio 45469

Earlier cytochemical studies in our laboratory involving lead precipitation techniques offered evidence that phosphodiesterase was located in the chloroplast lamellae and pellicle of Euglena while the adenylate cyclase was found in the outer chloroplast membranes. Subsequent biochemical assays have confirmed the location of phosphodiesterase in the pellicle. This phosphodiesterase has a pH optimum similar to that found in mammalian systems. When cGMP is used as substrate, its Km is lower than that obtained with cAMP as substrate. The specific activity of the plastid-associated phosphodiesterase appears to be different depending on the particular carbon source used in the growth medium. Biochemical assays for adenylate cyclase have been done on dark grown cells and the results of these assays indicate that adenylate cyclase is located in the flagella, in a fraction containing proplastids and in a microsomal fraction.

F-PM-B3 THE PRESENCE OF NUCLEOSIDE DI AND TRIPHOSPHATASE ACTIVITY ASSOCIATED WITH VARIOUS NUCLEAR SUBFRACTIONS. J. P. Perras and R. A. Menzies, * Life Sciences Center, Nova University, Fort Lauderdale, Fla., 33314.

In a previous communication (Federation Proceedings, 35(7), 1383, 1976)we reported the presence of nucleoside triphosphatase activity which exhibited multiple specificities from rat liver homogenates. The method of assaying for the presence of these enzymes has been changed. The present use of high resolution rapid chromatography (Hamilton HA-X10.00 anion exchange resin) detects the release of the several possible nucleotide products. The presence of nucleotide phosphatases with differing specificities, each yielding orthophosphate as one of the products, necessitates the resolution of the nucleotide products to distinguish between these enzymes. This approach has been used to study the nuclear distribution of guanine di and triphosphatase activities. Fractionation of nuclei from rat liver into various components, i.e., soluble, basic protein (histones), acidic nuclear proteins and nucleoli, results in the distribution of the diphosphatase and triphosphatase activity into specific subfractions. The majority of the diphosphatase activity is isolated in the soluble fraction and triphosphatase activities is distributed between the acidic nuclear protein and the nucleoli fractions. The presence within the nucleus of enzymes which hydrolyze the apparent precursors to DNA poses the problem of discovering the regulatory mechanism which would prevent a futile cycle. Supported in part by PHS Grant NIH-NCI CA15837.

F-PM-B4 ON THE MAXIMUM GROWTH RATE OF ESCHERICHIA COLI WITH SUCCINATE AS A SOLE CARBON AND ENERGY SOURCE. C. Houston Wang* and Arthur L. Koch, Microbiology Department, Indiana University, Bloomington, In. 47401

Derivatives of E. coli strains ML or B subcultured with succinate as the carbon and energy source, achieve balanced growth with doubling times of 60 min or greater. We have found that by further subcultures in low (0.02%) succinate, they will grow with doubling times of 25-31 min at 37°C. Cells growing rapidly in this medium can also be produced after a dozen doublings under succinate-limited chemostat culture. Under further chemostat culture the cells lose this capability. Measurement of β-galactosidase of lac operon constitutive strains indicate that the rapidly growing cells are severely catabolite repressed; on the other hand, the cells from long term chemostats have considerably higher levels of β-galactosidase than previously observed for presumably non-catabolite repressed succinate grown cultures of this strain. We believe that these two kinds of long term adaptations do not represent mutation and selection, but physiological states that may have ecological importance. Of special pertinence to the question of the control by the organism of the synthesis of various macromolecules is the finding that at a certain point in chemostat culture cells are present which very quickly shift from the slow growth rate of the chemostat to rapid growth without sufficient time to alter or form new macromolecules. This implies that an excess of unused, but quickly usable cellular components for all processes needed to grow rapidly are present in these slowly growing cells.

Work in this laboratory is supported fiscally and spiritually by the National Science Foundation metabolic biology program, BMS 72-01852 A03.

F-PM-B5 THE CONTRASTING OF POLYVINYLPYRROLIDONE (PVP-360) AND DEXTRAN (DX) AS ROULEAUX-INDUCING AGENTS. L.S. Sewchand* and P.B. Canham, Biophysics Dept., University of Western Ontario, London, Ontario, Canada.

The influence of the two rouleaux-inducing agents, polyvinylpyrrolidone (PVP-360) and Dextran (Dx-70, Dx-110, Dx-500), was contrasted by microscopic studies on erythrocytes from cat, rabbit and human. The average size of rouleaux as a function of the concentration of rouleaux-inducing agent increases to a maximum for human cells in Dx-Ringer and then decreases to unity at high concentrations. These results fit well with the theory of Chien and Jan (1) on macromolecular bridging. However cells from cat and rabbit did not demonstrate the disaggregation tendency at high Dx concentrations, and the agent PVP showed in contrast a monotonically increasing aggregating effect with increasing concentration for all types of cells tested. The results suggest that the binding of Dx molecules to the red cell surface varies with the species type, and that the bridging mechanism of PVP molecules is different from that of the Dx molecules.

(1) Chien, S. and Jan, K.M.: Microvasc. Res. 5:155 (1973)

(Supported by the Ontario Heart Foundation)

F-PM-B6 ZINC IONS AND TUBULIN ASSEMBLY. F. Gaskin, Depts. of Pathology (neuropathology) and Biophysics, Albert Einstein College of Medicine, Bronx, N. Y. 10461

Microtubules (MT) are in equilibrium with tubulin in vitro and the equilibrium data fits a nucleated condensation model. The assembly of MT is inhibited by Ca^{2+} and promoted by Mg^{2+},[1] whereas Zn^{2+} induces the formation of sheets of tubulin.[2,3] Turbidimetric measurements (A_{350}) were used to study the assembly kinetics of tubulin (0.8 to 2.2mg/ml) at 30°C in the presence of 0 to 1.0mM Zn^{2+}. As Zn^{2+} was increased, the lag time decreased, the rate increased and the plateau value increased. Protein determinations on samples centrifuged to pellet large aggregates showed an increase of protein in the pellet with an increase in initial Zn^{2+}. However, the amount of protein in the pellet was not proportional to A_{350}, except for those samples which assembled into MT. At 0.01mM Zn^{2+}, tube-like aggregates were frequently found by electron microscopy. Sheets of tubulin with 25-60 protofilaments oriented in parallel were found between 0.05-0.5mM Zn^{2+}. Above 0.5mM Zn^{2+}, non-specific aggregates were usually found. Increasing the Zn^{2+} added to MT resulted in more and more sheets and less and less MT. A_{350} and pelletable protein were also increased when Zn^{2+} was added to MT. The above studies were performed on tubulin prepared by the procedure of Shelanski, et al[4] and contains several MT associated proteins (MAP). Tubulin further purified by phosphocellulose chromatography and free of MAP will not form MT at 37°C using standard assembly conditions[5] but in the presence of 0.05-0.4mM Zn^{2+}, forms tube-like sheets about 250nm in diameter. ([1]Weisenberg (1972) Science 177, 1104. [2]Larsson, et al (1976) Exp. Cell Res. 100, 104. [3]Gaskin, et al, in press in Contractile Systems in Non-Muscle Cells, ed. Perry and Margreth. [4]Shelanski, et al (1973) Proc. Nat. Acad. Sci., 70, 765. [5]Weingarten, et al (1975) Proc. Nat. Acad. Sci. 72, 1858.

F-PM-B7 MICROTUBULE ASSEMBLY IN DEAE DEXTRAN: EFFECT OF CHARGE DENSITY AND MW OF THE POLYCATION. H.P. Erickson* and B. Scott*, (Intr. J. Corless) Duke Univ., Durham, N.C. 27710)

Polymerization of purified tubulin may be induced by a variety of polycations (PNAS 73:2813). We have prepared samples of DEAE dextran (Dd) with different charge density and MW, starting with dextran fractions of 2,000,000 MW (Pharmacia), as described by McKernan and Ricketts (Biochem. J. 76,117). The concentration of reagents was reduced up to fourfold for some preparations. Fractions of high MW(>120,000) were obtained by chromatography on Sepharose 6-B. The density of DEAE groups determined by Kjeldahl N analysis and H ion titration. Two samples had 0.38 and 0.7 meq/g, corresponding to one DEAE group per 16 and 8.5 glucose units. All of the charged groups were of one type, with pK_a = 9.5. Commercially available Dd (Pharmacia) is more highly charged (2 meq/g) but about half of the DEAE substituents are present as "tandem"groups", giving a complicated mixture of single and double charges,with different pK_a's. In assembly experiments the most striking observation was that our synthesized Dd induced only normal MTs, which were generally found in closs-packed, parallel bundles of 2 - 20 MTs, while Pharmacia Dd produced only "double-wall" MTs. These aberrant forms may therefore be due to the higher charge density or to the tandem groups. Pelleting assay indicated that the assembly was limited primarily by the total number of DEAE groups added, the stoichiometry being 8,9.4 and 12 DEAE groups per 55,000 MW tubulin subunit for the 3 samples (0.38, 0.7 and 2 meq/g). With high MW Dd fractions 80 % of the tubulin could be assembled, while 20,000 MW fractions gave up to 60 % assembly. One fraction of low MW and low charge, having fewer than 8 DEAE groups per Dd molecule, gave virtually no assembly. Thus MT assembly in this system may require a polycation to neutralize 10 charges per tubulin subunit, and large enough to span at least two subunits.

F-PM-B8 COMPUTER SIMULATION OF CELLULAR MOVEMENTS. N.S. Goel , and G. Rogers*, School of Advanced Technology, State University of New York, Binghamton, N.Y. 13901

Using a model proposed earlier by one of the authors (NSG) and a set of plausible motility rules, a computer simulation of engulfment of two or more intact embryonic tissues has been successfully carried out. Same motility rules have been used to simulate the rounding up of a tissue, centralization of one tissue within another tissue, a process analog to differentiation, phenomenon of cell-sorting, migration of individual cells through tissues and contact inhibition of overlapping. The simulations in most part are found to be consistent with the observations with real cells. The computer software, in conjunction with an appropriate hardware configuration, allows a visual display in color of the dynamics of cellular movement.

F-PM-B9 AN OPTIMAL CONTROL STUDY OF THE IgM-IgG SWITCH. A. S. Perelson,* S. Rocklin,* and B. Goldstein, Theoretical Biology and Biophysics Group, Theoretical Division, University of California, Los Alamos Scientific Laboratory, Los Alamos, New Mexico 87545.

For a large class of antigens, during a primary response, the immune system first produces IgM antibodies and then switches to the production of IgG antibodies. The evolutionary rationale for switching the class of immunoglobulin secreted is investigated through the use of control theoretic models. An optimal control problem is formulated in which the objective is to minimize the time it takes to reduce a proliferating antigen to a safe level. In particular, the efficacy of IgM and IgG in complement dependent lysis of pathogenic organisms is examined. Strategies in which there is secretion of only IgM, only IgG, and IgM followed by IgG are compared.

This work was performed under the auspices of U. S. Energy Research and Development Administration.

F-PM-B10 A STEP INCREASE IN NERVE MICROVISCOSITY AT THE TEMPERATURE CAUSING COLD BLOCK OF FAST AXOPLASMIC TRANSPORT. R.A. Haak, F.W. Kleinhans‡ W.J. Newhall, and S. Ochs, Medical Biophysics and Physics (IUPUI), Indiana University School of Medicine, Indpls., IN 46202

A spin label ESR investigation of nerve with relation to fast axoplasmic transport has shown that cat sciatic nerve axoplasm has a microviscosity approximately 5 x that of water (Haak, R.A., Kleinhans, F.W. and Ochs, S., J. Physiol., in press). This result was based on the observed decrease in the rotational diffusion of the low molecular weight spin probe tempone in the nerve as compared to water. Localization of the label signal to the axoplasm was accomplished with Ni^{2+}. Data taken using grouped samples showed that over the range from 38°C to 0°C, τ_c increased in a manner similar to H_2O. This result was used to exclude a large increase in viscosity at temperatures below 11°C as the cause for the phenomenon of cold block of fast transport. However, data taken from single nerves as the temperature was varied from 25°C to 5°C showed a small, reproducible, step increase in τ_c at close to 11°C, the temperature at which cold block occurs. This effect was absent in nerves pretreated with 3 mM vinblastine, a vinca alkaloid known to block fast transport. The step in τ_c was also absent when nerves were initially exposed to cold and not allowed sufficient time for recovery. Vinblastine treated nerves bathed in an isotonic D_2O sucrose solution showed the step, and it was not detected when 20 mM Ca^{2+} was added. The step may be related to a disassembly of microtubules treated with vinca alkaloid or exposed to low temperature. The physical basis by which a microtubular disassembly process can cause the step increase in viscosity remains to be determined.

(Supported in part by Research Corporation and NSF Grant No. BNS 75-03868-A02.)

F-PM-B11 INTRACELLULAR SELF DIFFUSION OF WATER IN LIVING CELLS. J.E. Tanner, Naval Weapons Support Center, Applied Sciences Department, Crane, IN 47522.

Self diffusion of water has been measured in live frog muscle, and in packed-cell samples of yeast, E. coli and human red cells over an extremely wide range of diffusion times, using pulsed-field-gradient, spin-echo NMR. The intracellular diffusion coefficient, at measurement times short enough so that the effect of the cell membrane can be resolved (approximately 0.5 msec), is about 1.6×10^{-5} cm²/sec for frog muscle and $5 \pm 1 \times 10^{-6}$ cm²/sec for the packed cell samples. When measured over times long enough to allow penetration of the cell membranes (0.5 to 2 sec.) the apparent diffusion coefficient decreases by a factor of x1.5 or more, depending on the type of sample. From the diffusion data, a membrane permeability of 0.02 cm/sec was estimated for the red cells and for the frog muscle cells. The permeability of E. coli membrane is much higher. $T_1 \gg T_2$ in all samples, consistent with a small fraction of relatively immobile water.

The cell samples and helpful discussions were furnished by Professor Al Strickholm, Department of Physiology; Professor Henry Mahler, Department of Chemistry; and Professor Arthur Koch, Department of Microbiology; and their students, at Indiana University, Bloomington, Indiana 47401.

This work was supported by the Office of Naval Research, Contract N0001477WR70035.

F-PM-B12 THE ACTIVITIES OF CYTOPLASMIC SODIUM AND POTASSIUM. S.B. Horowitz, L. Tluczek*, and P.L. Paine*, Cell Physiology Laboratory, Michigan Cancer Foundation, Detroit, MI 48201.

A new approach to determining the activity of cytoplasmic Na^+ and K^+ is described. Liquid gelatin (35°C) is injected into an amphibian oocyte, then gelled (0°). Incubation (15°C) allows diffusional equilibration of Na^+ and K^+ between the gel and cytoplasm. The cell is then frozen in liquid N_2 and the gelatin and cytoplasm isolated by microdissection at temperatures low enough to prevent ion redistribution. Analysis is by flame emission spectroscopy. In the oocyte of *Desmognathus ochrophaeus*:

	µEq Na^+/ml H_2O	µEq K^+/ml H_2O
cytoplasm	48.3 ± 2.2	97.2 ± 4.1
gelatin	16.0 ± 3.4	124.0 ±13.1

Activities are determined by reference to known aqueous solutions using gelatin/water dialysis. We conclude that: 1) The activity coefficient of Na^+ in cytoplasm is less than that in an aqueous solution of the same concentration, implying Na^+ sorption or sequestration by cytoplasmic elements. This result agrees with those obtained using isotopic exchange techniques (Century & Horowitz, 1974, J. Cell Sci. 16:465) and ion-selective microelectrodes (Dick and McLaughlin, 1969, J. Physiol. 205:61). 2) The activity of cytoplasmic K^+ is greater than in comparable aqueous solutions--a fact not disclosed by electrode studies (ibid.) but consistent with observed solute exclusion by cytoplasmic water (Horowitz & Paine, 1976, Nature, 260: 151).

Supported by NIH grant GM 19548 and an institutional grant from the United Foundation of Greater Detroit.

F-PM-B13 A POTENTIAL MODULATOR OF NOREPINEPHRINE ACTION (A GLYCOPEPTIDE). C.Torda, N.Y. Center for Psychoanalytic Training & Mt.Sinai Sch.Med., 10 E. 100 Str.,N.Y.,N.Y.,10029.

The discrepancy between catecholaminergic functions and number of specific receptors in some intracerebral regions prompted the search for modulator substances. Since norepinephrine dependent functions ofimmature hypothalamic dendrites are largely supported by a glycoprotein fraction (C.Torda, J. Neuroscience Res., 2, 21, 1976), isolated by C.L.Lee (Brain Res., 81, 497, 1974), the potential modulator property of this substance on functions of norepinephrine-dependent systems has been studied in the present work: 1) Frequency changes of spontaneous activity of Purkinje cells (G.R.Siggins, B.J.Hoffer & F.E.Bloom, Brain Res., 25, 523, 1971), and 2) norepinephrine-related properties of induced aggressive behavior served as test objects. The effects of this glycoprotein fraction were measured in presence of local enrichment of exogenous or endogenous norepinephrine, or tissue depletion of endogenous norepinephrine by various methods. The results led to the conclusion that this glycoprotein fraction fulfills the minimum necessary requirements of a modulator of the effects of norepinephrine: e.g.1)in physiological concentrations this glycoprotein fraction lacks neurotransmitter effect; 2) its affinity (binding power) for norepinephrine is considerable; 3) it potentiates the effects of norepinephrine in vivo (in a different manner than the effects of other catecholamines so far tested); and 4) prolongs the effect of norepinephrine far beyond termination of endogenous release or excessive local availability of norepinephrine.

F-PM-B14 ACETYLCHOLINE, CALCIUM, AND CYCLIC NUCLEOTIDES IN THE CELLULAR CONTROL OF PEPSINOGEN SECRETION. D.E. Schafer, Veterans Administration Hospital, West Haven, and Department of Physiology, Yale University School of Medicine, New Haven, Conn. 06510.

In the gastric mucosa, the sites of macromolecular biosynthesis and the stimuli for exocytosis vary considerably with species. The only known physiological stimulus for pepsinogen secretion (PS) in the rabbit is acetylcholine (ACH). We have investigated some possible intracellular mechanisms of PS *in vitro*, using strips of rabbit gastric mucosa in the presence or absence of ACH (10^{-4} M, plus eserine). Although omission of Ca^{++} from the medium inhibits the ACH-stimulated secretion of total ^{14}C labeled protein by the mucosa, omission of Ca^{++} for up to 4 hr caused only a statistically insignificant inhibition of ACH-stimulated PS; if, in addition, Sr^{++} (2 mM) was present, PS was inhibited significantly. The ionophore X537A (25 µg/ml) stimulates PS by 275% over basal, but A23187 (1 µg/ml) had no stimulatory effect. Veratridine (10^{-4} M) caused an 82% increase in PS. Analogs of cyclic GMP failed to stimulate PS, whereas 1 mM 8-Br cyclic AMP produced a 120% stimulation, and 2 mM dibutyryl cyclic AMP stimulated PS maximally. 10^{-3} M IBMX also evoked maximal PS, and 10^{-4} M IBMX was nearly as effective. To date, no consistent change in gastric mucosal levels of either cyclic nucleotide has been observed in the presence of ACH, over a wide range of incubation times. On the other hand, 10^{-3} M IBMX produces a striking increase (16-fold) in cyclic AMP levels and a 2 1/2 fold rise in cyclic GMP levels within 15 min. These results suggest that, as in many other systems, calcium plays a role in stimulus-secretion coupling in the case of ACH-stimulated PS in the rabbit, and that mechanisms exist whereby cyclic AMP or, conceivably, cyclic GMP may induce PS. As yet, however, neither cyclic nucleotide is implicated in the PS-stimulatory action of ACH.

F-PM-B15 CATION REQUIREMENT FOR SPERM BINDING TO THE ZONA PELLUCIDA OF THE MOUSE. P.M. Saling, B.T. Storey and D.P. Wolf*, Depts. of Physiology and Obstetrics & Gynecology, University of Pennsylvania School of Medicine, Philadelphia, PA 19174.

Epididymal mouse sperm may be capacitated *in vitro* (Inoue and Wolf [1975] Biol. Reprod. 13:340) in a defined culture medium (CM) of inorganic salts, lactate, pyruvate, glucose and serum albumin. Sperm so capacitated bind to the zona pellucida; uncapacitated sperm do not (Wolf and Inoue [1976] J. Exp. Zool. 196:27). The minimal requirements for reactions leading to capacitation may be defined with this binding assay. Superovulated, cumulus-free eggs from Swiss albino mice were inseminated *in vitro* with epididymal sperm preincubated for 1 hr at 37° in: a) CM; b) Tris (20 mM)/NaCl (130 mM), pH 7.4 (TN); or c) Tris (20 mM) /NaCl (125 mM) / $CaCl_2$ (2 mM), pH 7.4 (TNC). The ova were recovered, washed and fixed in one step via centrifugation through a discontinuous Dextran/Dextran-gluteraldehyde gradient at 30, 60 and 90 min post-insemination, and examined for sperm binding after staining with aceto-lacmoid. Ova in TN medium inseminated with sperm ($1\text{-}2 \times 10^5$ sperm/ml) preincubated in either CM (1.71 mM Ca^{+2}) or TNC (2.0 mM Ca^{+2}) have a mean of at least 2 sperm bound per zona. The TN-preincubated sperm do not bind to the zona, although they remain motile throughout the experiment. Ca^{+2} is thus required by the sperm to acquire the ability to bind to the zona. La^{+3} does not inhibit the Ca^{+2} effect; it enhances it slightly and substitutes for Ca^{+2} at 5 µM, which eliminates the possibility that the transport of Ca^{+2} into the sperm cell is the primary mechanism of the Ca^{+2} effect. EGTA (2 mM), when added to the CM sperm suspension 30 min prior to insemination, reduces the level of sperm binding to that observed with the TN medium. The data suggest that a change in cell surface charge, due to the reversible binding of Ca^{+2} to the plasma membrane (for which lanthanide cations may substitute), is essential for sperm binding to the mouse zona pellucida. (Supported by USPHS HD-06274, HD-07635 & 5T01-00205-17).

F-PM-B16 CALCIUM WAVE DURING ACTIVATION OF MEDAKA EGGS. J.C. Gilkey*, E.B. Ridgway, L.F. Jaffe, and G.T. Reynolds. Purdue University, West Lafayette, Indiana 47907, Medical College of Virginia, Richmond, Virginia 23298, and Princeton University, Princeton, New Jersey 08540.

Aequorin-injected Medaka eggs show a dramatic calcium-transient on activation by sperm. Using image intensification techniques, it is possible to show that the calcium transient on activation is due to a spreading calcium wave. The wave is initiated at the micropyle and then spreads over the remaining surface of the egg, finishing at the vegetal pole. Ionophore (A23187) activated eggs show multiple initiation sites, and the calcium waves annihilate each other where they meet. The velocity of propagation of the calcium wave is faster over the animal hemisphere than over the vegetal hemisphere. Propagation of the wave is apparently not dependent on external calcium since eggs suspended in 40 mM Mg, 1 mM EGTA show normal waves. Evidently, the calcium wave is self-propagating and involves some kind of calcium-mediated calcium release from internal sources. The relationship between the calcium wave and the well known wave of cortical vesicle breakdown (secretion) was followed by making alternating image intensifier photographs and light micrographs. The calcium wave precedes cortical vesicle breakdown.

F-PM-C1 FLUORESCENCE POLARIZATION EXPRESSIONS: CORRECTIONS FOR THE LIMITED VIEW OF THE OBSERVER. R. M. Dowben and W. A. Wegener*, Departments of Biophysics and Physiology, Univ. Texas Health Science Center, Dallas, Texas 75235.

Fluorescence polarization is a widely used method for studying the size, shape, and even orientational properties of macromolecules. The theoretical expressions developed have always considered the probability an excited fluorophore would emit a photon along various laboratory axes. Experimentally, however, a photon must be detected, and therefore, the probability for emission in the direction of the observer must be taken into account if theory and experimental observations are to be related accurately. We will refer to the general theoretical expressions that take into account the limited purvue of the observer as conditional expressions.

General conditional expressions are developed; their qualitative and limiting properties are explored. For certain oriented distributions of fluorophores, explicit results are calculated and compared with the general theoretical expressions which ignore the role of the observer. For time-dependent fluorescence polarization, the conditional time-dependent intensities are derived for the case of arbitrary absorption and emission dipoles rigidly fixed to a general ellipsoidal body. The resulting conditional anisotropy function is compared to the general anisotropy function. We also calculate the conditional steady-state polarization expressions and compare them with the previously derived general expressions.

Supported by grant HL-16678 from the National Heart, Lung, and Blood Institute.

F-PM-C2 SOME MODELS OF CURRENT FLOW IN ELECTRICAL SYNCYTIA. Eric Jakobsson, Lloyd Barr, & Russell McKown*, Dept. of Physiol. & Biophys., U of Illinois, Urbana, Illinois 61801.

We are using both lumped parameter and continuous function models to predict electrical behavior of tissues whose cells are interconnected by nexuses. A radial patch model previously developed for nodes of frog heart muscle in double sucrose gap voltage clamp experiments (Jakobsson, et al., Biophys. J. 15:1069) has been improved by making finer the "mesh size" for spatial integration in the radial direction. We find that the observed and simulated voltage clamp current wave forms now come into very close agreement, except for the experimentally observed "abominable notch" which depends on current size and node width, thus suggesting that, except for the notch, the differences between heart muscle and axonal rapid transient current records are due to the high resistance to extracellular current flow in the radial direction. To deal with notching, longitudinal and radial intracellular resistances are being added. Responses to sinusoidal input of both the model and the tissue are being explored. The continuous function modelling assumes that the cell membrane is homogenously distributed in space and is the boundary between coextensive intracellular and extracellular spaces whose resistances along one axis differ from those in the other two dimensions by a factor. Computations of the electrotonic spread in a tissue due to step and sinusoidal currents imposed between two points on either side of a cell membrane were made using the solutions: Step: $V_m = \frac{C}{\sqrt{p}} \exp\left[-\sqrt{p}/\lambda_r\right] \operatorname{erfc}\left(\sqrt{(\rho C_m)/(t G_m)}/(2\lambda_r) - \sqrt{t G_m / C_m}\right)$

Sinusoid: $V_m = \frac{C}{\sqrt{p}} \exp\left[i\omega t - \sqrt{p}/\lambda_r'\right]$ where $C \equiv I_T/(8\pi\lambda_r\lambda_z G_m A_m)$;

$\lambda_r' \equiv (G_m A_m - i\omega C_m)^{-1/2} (R_{o,r} + R_{i,r})^{-1/2}$ other symbols as defined in Barr & Jakobsson p. 41 Physl. of Smooth Muscle, Raven, 1976.

F-PM-C3 POTENTIAL PROFILES AND EQUILIBRIUM DISTRIBUTION OF IONS WITHIN A POLARIZED SPHERICAL SHELL. G. M. Schoepfle and W. S. Rehm, Department of Physiology and Biophysics, University of Alabama in Birmingham, The Medical Center, Birmingham, Alabama 35294

Solutions of the Poisson-Boltzmann equation yield potential profiles and equilibrium distributions of ions on either side of a spherical shell membrane across which there exists a separation of free ionic charges. Within the sphere charge density is approximated with less than 0.1% error by the formulation $\rho = \Sigma F[C_i][1 - z_i F(V-V_1)/RT]$ where C_i and z_i define concentration and valence of the i th monovalent ion. V is the potential at any point defined by the radius r for all $r_1 < r < b$ within a spherical shell membrane of inner radius b. Radius r_1 is that of a very small concentric sphere which encloses no free charge. Since dV/dr is equal to $d(V-V_1)/dr$ the Poisson-Boltzmann equation may be expressed as $d^2(V-V_1)/dr^2 + (2/r)d(V-V_1)/dr = (V-V_1)/D^2$ in which $D^2 = [e_w RT/4\pi CF]$, e_w is the dielectric constant of water and C is the sum of anionic and cationic concentrations. The desired particular solution assumes the form $V-V_1 = [A/r][\exp(r/D) - B\exp(-r/D)]$ where B is assigned the value $\exp(2r_1/D)$ in order that $V-V_1$ may vanish at r_1. The remaining arbitrary constant must then be given as $A = [-qD/e_w][(b-D)\exp(b/D) + B(b+D)\exp(-b/D)]$ in which q is net free charge enclosed within the entire sphere. For any radius r_2 which defines a point at which charge density is finite the electric field -dV/dr is determined only by the total charge enclosed within a sphere of radius r_2. However, free charges outside this sphere will determine in part the ionic diffusion gradient for any particular ion at r_2. Total moles M_i of the i th ion within the sphere is expressed as the sum of the contributions enclosed in contiguous shells of thickness dr and volume $4\pi r^2 dr$. As an approximation $M_i = [C_i][(4\pi b^3/3) + (z_i q/FC)]$ where q/FC may be envisioned as an "equivalent volume" occupied by the ion in question. NIH support.

F-PM-C4 THERMODYNAMIC MODEL OF THE KINETICS OF WATER LOSS FROM CELLS FROZEN BY A "TWO-STEP" PROCEDURE. W. F. Rall[*1] and Peter Mazur, Univ. of Tenn.-Oak Ridge Graduate School of Biomedical Sciences and Biology Div., Oak Ridge National Lab., Oak Ridge, Tenn. 37830

Cells cooled too rapidly are believed to be killed by intracellular freezing. Previously a thermodynamic relationship was developed which describes the kinetics of cell dehydration during freezing (Mazur, J. Gen. Physiol. 47:347, 1963). This relationship is described by a set of differential equations giving cell water content as a function of temperature, cooling rate, cell surface area-volume ratio, cell membrane permeability to water, and temperature coefficient of the permeability coefficient. The calculated cell water content permits predictions of the likelihood of intracellular freezing, and these predictions have been confirmed. We now describe a modification of this earlier thermodynamic model allowing calculation of the kinetics of cell dehydration when cells are frozen using a "two-step" procedure. This procedure has yielded high survival of several cell types after thawing and provides a powerful cryobiological tool (Farrant et al., Nature 249:452, 1974). In two-step freezing, rapid cooling to -196°C is interrupted with a timed exposure at an intermediate temperature (usually ~ -25°C). Cell survival has been found to be dependent on the time of exposure at the intermediate temperature. We have calculated the cell dehydration behavior of Chinese hamster tissue culture cells and other cell types during two-step freezing and have predicted the likelihood of intracellular freezing. Both the calculated water contents and predictions of intracellular freezing are consistent with the experimental observations of Farrant and his colleagues. The protective effect of time during the interruptive step of two-step freezing can be explained in terms of sufficient cell dehydration to preclude intracellular freezing. (Research sponsored by ERDA under contract with the Union Carbide Corp. [1]Predoctoral Fellow supported by grant GM 1974 by NIGMS, NIH.)

F-PM-C5 STOCHASTIC THEORY OF BIMOLECULAR CHEMICAL REACTIONS. A.K. Thakur*, C. DeLisi, and A. Rescigno†, Laboratory of Theoretical Biology, National Cancer Institute, National Institutes of Health, Bethesda, Maryland 20014

A stochastic model of the bimolecular reversible reaction $2A \rightleftharpoons C$ is formulated on Markovian assumptions. The forward Kolmogorov equation for the probability distribution is found to be $dP_i(t)/dt=(\alpha/2)(i+1)(i+2)P_{i+2}(t)+(\beta/2)(N-i+2)P_{i-2}(t) - [(\alpha/2)i(i-1) + (\beta/2)(N-i)]P_i(t)$ ... (1) where α and β are the forward and backward reaction rates, i is the number of molecules of type A at any time t and $N(\equiv 2A+C)$ is the total number of units in the system at all times (conserved). The exact equilibrium distribution function is found by a combinatorial method to be $P_{2n}(\infty)=[(N/2)(N/2-1)\ldots(N/2-n+1)K^n]/[(n!)\{2n-1)!!\}\mathcal{Z}]$ where $\mathcal{Z}$ is the partition function $= 1 + \sum_{n=1}^{[N/2]} \Omega(N,n)K^n$ with $\Omega(N,n)=[(N/2)(N/2-1)\ldots(N/2-n+1)]/[n!(2n-1)!!]$. Moments obtained from the numerical solution of (1) agree satisfactorily with those found by truncations. The results led to the reconstruction of the kinetic distribution on the Normal basis set using Hermite Polynomials. Use of only the first four moments in this expansion produced excellent approximation for the distribution both near and far from equilibrium.

F-PM-C6 THE UNCERTAINTY ASSOCIATED WITH OUABAIN BINDING CONSTANTS FROM SCATCHARD PLOTS. F. Mandel, Department of Cell Biophysics, Baylor College of Medicine, Houston TX 77030

The exact expression for the percent binding, B, of a substrate, S, to an enzyme containing two different binding sites is:

$$B = \frac{X[S] + 2Y[S]^2}{1 + X[S] + Y[S]^2} \qquad (1)$$

where $X = K_1 + K_2$ and $Y = K_1 K_3$. The K's are the three independent binding constants ($K_4 = K_1 K_3/K_2$) of this system and may or may not be equal. Eq. (1) shows that B is dependent solely on the values of X and Y. Thus, any three constants resulting in the same X and Y will yield the same B and hence the same Scatchard plot. A single set of data can therefore be interpreted as sites having negative cooperativity, positive cooperativity, or lacking cooperativity. This means that neither the degree of cooperativity nor the heterogeneity of the sites may be inferred from the curvature of a Scatchard plot or any other plot using the binding data. Often Scatchard plots are analyzed by a least squares fit of:

$$B = \frac{a[S]}{1 + a[S]} + \frac{b[S]}{1 + b[S]} \qquad (2)$$

Eq. (2) is identical to Eq. (1) with $a + b = K_1 + K_2$ and $a\,b = K_1 K_3$. Thus, regardless of the cooperativity or homogeneity associated with the enzyme, a good fit always results (except when the K's are such that a and b must be complex numbers. Conversely, a poor fit may be due to the arbitrary restriction that a and b are real numbers. The basic problem is that while there are three independent binding constants, binding studies yield only two pieces of information. The resulting ambiguity can not be resolved by binding studies alone but requires an additional experiment such as the calorimetric determination of ΔH. (Supported by NIH Grant #HL 07219.)

F-PM-C7 MOLECULAR KINETICS IN NEUROPHYSIOLOGY, Okan Gurel, IBM Corporation, 1133 Westchester Avenue, White Plains, New York 10604.

Two basic concepts of neurodynamics are presented. The first one, the "spike concept" has been extensively implemented in the experimental neurophysiological studies. Chemical kinetics models of Rossler (1,2) will be used to illustrate the theoretical basis of spike realization in neurodynamic systems. The second concept of "coil" formation is more complicated, however, this opens up a new dimension in neurophysiology, Gurel (3). Dynamic realization of this idea as a kinetic model is provided in the recent papers by Rossler (1,4). These examples are results of the concept of partial peeling (5). Implications of both the spike and the coil formations are yet to be explored in understanding the role of molecular dynamics in neurophysiology.

(1) O. E. Rossler, Chaotic Behavior in Simple Reaction Systems, Z. Naturforschung, 31a, (1976) 259-264.
(2) O. E. Rossler, An Equation for Continous Chaos, Physics Letters, 57a (1976) 391-392.
(3) O. Gurel, Topological Dynamics in Neurobiology, Intrn. J. Neuroscience, 6 (1973) 165-179.
(4) O. E. Rossler, Chaos in Abstract Kinetics: Two Prototypes, Bull. Math. Biol. (in press).
(5) O. Gurel, Partial Peeling, In: Dynamical Systems 2 (L. Cesari, et al. Eds.), Academic Press, Inc. New York (1976) 255-259.

F-PM-C8 LOW MOBILITY BIOENERGENTICS. W. Moorhead*, J. McGinness*, and R. Shalek, M. D. Anderson, Houston, Texas 77030

The experimental discovery of amorphous semiconductor switching in cytochrome c (equine) indicate that these materials are capable of functioning as exotic electronic devices. The purpose of this abstract is to suggest that the low mobility of electronic conduction in these and other biological materials, which has been considered to be a major empediment to the application of solid state concepts to materials which are such poor conductors, may allow a degree of microminiturization which is not possible in high mobility materials. Our model for electron transport is the quantum langevin equation in the Heisenberg representation.

$$\frac{d\hat{V}(t)}{dt} = -\beta\hat{V}(t) + F + \hat{D}(t)$$

We suggest the use of a delta function, which is standard, plus the derivative of a delta function which to the best of our knowledge commences with this abstract.

$$\langle \hat{D}(t_1)\hat{D}(t_2)\rangle = A(T)\delta(t_1-t_2) + B\frac{d}{dt}\delta(t_1-t_2)$$

This choice is based on the observation that the resulting solution for the spread of the electron wavepacket from its initial localization

$$(\Delta x)^2 = L^2/2 + [\hbar/mL\beta]^2(1-e^{-\beta t})^2 + A(T)t/\beta^2$$

reduces to a temperature independent form obtained by Buch and Denman while avoiding problems with the uncertainty principle which prevented direct application of their results. The spread in the wavepacket is minimum in a low mobility material allowing independent charge transfers to occur in a smaller volume than would be possible in a higher mobility material. Furthermore materials which follow a compensation law behavior possess a particular advantage if the mobility and number of carriers are inversely related. Finally, low mobility appears to be a requirement for the paired moving charge model of Bioenergetics.

F-PM-C9 THE DISTRIBUTION OF TRANSIT TIMES IN A FLOWING STREAM AND THE VALIDITY OF THE PLUG-FLOW ASSUMPTION. K.-H. Chen*, W. Siler*, and K. Burchfield*. (Intr. by J. Macy), Department of Biomathematics, University of Alabama in Birmingham, Birmingham, Alabama 35294

In modelling the degradation of biological oxygen demand substrates in water pollution studies, the assumption is universally made that the water moves downstream with constant transit time between shore points. However, dye tracer studies show that there is considerable right-skewed dispersion of transit times. A model is presented to account for this dispersion using a combination of diffusion and mass-action transport which fits experimental data well. The model differential equations are solved analytically. This model is then used with the Streeter-Phelps equations for BOD degradation and deoxygenation to predict BOD and dissolved oxygen downstream from a pollution source, and the results compared with the plug flow model. The conclusion is reached that in most cases the plug flow model is adequate.

F-PM-C10 THE DYNAMICS OF A CELLULAR POPULATION MODEL: FROM STABLE EQUILIBRIA TO PERIODIC ATTRACTORS AND CHAOS. Michael C. Mackey, Departments of Physiology and Biomedical Engineering, McGill University, Montreal, Canada. H3G 1Y6

The development of a fully age structured resting phase cell cycle model under mitotic inhibitory control leads to a pair of coupled non-linear first order differential equations with time delays describing the time evolution of the proliferating and non-proliferating cells. Numerical and analytical studies indicate that increases in the inhibitory feedback sensitivity, the time delay, or the maximal mitotic rate, or a decrease in the cellular death rate, are capable of destabilizing an asymptotically stable equilibrium point. The locations in parameter space at which this occurs may be calculated exactly. Once this destabilization has occured, an (apparently global) periodic attractor appears, and the period of the solutions can be calculated exactly. Further changes in the parameters lead to the destabilization of the periodic solutions, and the appearance of 'strange attractors' and their attendant aperiodic solutions. The peculiar dynamics of chronic granulocytic leukemia are discussed in light of these behaviours with illustrative examples from the clinical literature.

Supported by the National Research Council of Canada, Grant NRC-A-0091.

F-PM-C11 QUASIPERIODIC OSCILLATION IN AN ABSTRACT REACTION SYSTEM. O.E. Rössler, Division of Theoretical Chemistry, University of Tübingen, Auf der Morgenstelle 8, D-7400 Tübingen, W. Germany.

A two-variable abstract chemical oscillator of Dreitlein-Smoes type becomes a quasiperiodic oscillator under an appropriate coupling with a third variable. In dependence on a single parameter, the obtained system shows either limit cycle behavior, or quasiperiodic behavior, or different types of nonperiodic behavior. The equation has the asset of being especially transparent analytically. It is a prototypic equation for other physico-chemical systems. The occurring bifurcations between quasiperiodic and chaotic behavior are similar to those in turbulence generation.

F-PM-C12 PRINCIPLE OF MOLECULAR ADAPTABILITY. M. Conrad, Dept. of Computer & Communication Sciences, University of Michigan, Ann Arbor, Michigan 48109.

The principle of molecular adaptability is: stepwise changes in the primary structure of proteins are often associated with gradual changes in their biological function, where the degree of gradualism is itself adjusted in the course of evolution. The principle is based on both biophysical and evolutionary considerations. The biophysical consideration is that biological function (catalytic specificity, self-assembly) depends on three-dimensional shape and that this is determined in the main by weak interactions among many amino acids, and therefore ultimately by primary structure. As the redundancy of weak interactions increases (for example, by the addition of amino acids whose sole contribution to function is to provide such redundancy) the shape and therefore function of the protein changes more slowly with single (but noncritical) changes in primary structure. Thus the degree of gradualism with which function changes with primary structure is itself a property of primary structure. The evolutionary argument is that evolution proceeds most rapidly when stepwise changes in structure are associated with small changes in function, and in general proceeds very slowly in all other cases. The principle of molecular adaptability results from the fact that the degree of gradualism is thus both a condition and consequence of evolution by variation and natural selection, so that those species whose complement of protein molecules are most suitably adjusted for evolution inevitably predominate in the course of evolution. The principle has implications for the interpretation of protein structure and for the relation of structure to function in a number of biological processes in which gradual function change is important. It also serves as a useful postulate for simulation studies of biological systems in which macromolecular processes play a critical role.

F-PM-C13 A STOCHASTIC MODEL OF OVIDUCTAL EGG TRANSPORT. P. Verdugo, W.I. Lee, R.J.Blandau* and S.A. Halbert, Center for Bioengineering and Department of Biological Structure, University of Washington RF-52, Seattle, Wash. 98195

A mathematical description of the relationship between apparent movements of the ovum in the Fallopian tube and the various forces generated by the mechanical effectors of this organ will be presented. Within the framework of a stochastic approach, we have used Langevin's equation to formulate a description of tubal transport which is deduced from qualitative features of this phenomenon rather than induced from numerical fitting of experimental data. We show that the egg transport in the tube can be represented as a one-dimensional random walk in a field of external force. The motion of the egg can be described by:

$$m \frac{dv}{dt} = -fv + A(t) + F \qquad (1)$$

Where v is the velocity of the egg. The influence of the intraluminal forces on the motion of the egg are represented by: a frictional force -fv; a randomly fluctuating force A(t), generated by the muscle component of the oviductal wall; and the driving force F generated by cilia. Accordingly the description of egg transport in terms of the probability distribution of ovum positions along the tube has the general form of Fokker-Plank equation. The specific constrants of the model provide the identification and characterization of the mechanisms involved and predict the various potential alternatives for physiologic regulation of the egg transport processes.

Supported by USPHS Grant GM-1643 and Contract HD3-2788

F-PM-C14 DESCRIPTION OF LONGITUDINAL BONE GROWTH. Larry A. Spitznagle,* Richard P. Spencer. Department of Nuclear Medicine, University of Connecticut Health Center, Farmington, Connecticut 06032.

Description of the growth in length of a bone must take into account 3 main factors. These are: I. The initial length of the bone (B_0, that at birth). II. The rate of growth. III. The final length. Hence, the equation can be of the form $L = B_0 + Q$. The term Q contains rate information as well as possible equilibrium data. While there are several possible approaches, a modified exponential gives a good description of the available data. For example, we can use this to quantify the growth of the ilium in domestic cockerels, using the raw data of Harrison (J. Anat. 109:63, 1971). The length (L, in mm) is given as the sum of the length at birth and that due to the growth term (t is in days). Thus: $L = B_0 + B\ (1 - e^{-\lambda t})$, where B is the value of $L - B_0$ at infinite time, and λ is the rate constant with the dimension of reciprocal days. For the cockerel ilium, the equation is: $L = 27 + 85\ (1 - e^{-0.0133t})$. The half-time for the growth phase is ln 2/rate constant, or 0.693/0.0133 = 52 days. At day 52, the ilium has a length of 27 + 85(½) or 70 mm. A related expression has been used in defining another event in bone, the growth of sternal ossification (Spencer, Biol. Neonat. 14:341, 1969). In disordered growth, such equations allow us to separately look at the initial length, the final length, and any alteration of the growth rate. Supported by USPHS CA 17802 from the National Cancer Institute.

F-PM-C15 BIOLOGICAL EXTINCTION AND THE STRUCTURE OF $W^s(0,f)$ FOR ITERATES OF C[0,1] MAPPINGS OF RESTRICTED FORM. Matthew Witten, Department of Biophysics, State University of New York at Buffalo, Buffalo, New York 14226

The structure of the extinction set $\mathcal{E}_f = \bigcup f^{-n}(0)$ for a function $f:[0,1] \to [0,1]$ is discussed. One form of an existence theorem is stated, and various common biological mappings are examined to determine the existence of $\mathcal{E}_f$. Also determined is the existence of a minimal zero stable subset $\mathcal{E}_0$. Examples of mappings whose extinction sets are of different structures are illustrated and discussed. The link between this formulation of the problem and problems in differential dynamics is discussed. It is shown that $\mathcal{E}_f$ is equivalent to the stable manifold of zero for a given f. Techniques from differential dynamics are applied to obtain classifications of topological semiconjugacies of mappings. Biological ramifications of the topological semiconjugacy theorem are discussed. This problem arises from evolutionary considerations as well as biological modeling considerations.

F-PM-C16 THE ORIGIN OF LIFE ON EARTH, Eliot M. Simon, Institute for Theoretical Physics, Free University of Berlin, Berlin, West Germany.

There have been numerous approaches to the problem of the origin of life on earth. The fact that the simplest biological cell contains an enormous number of organelles and interacting macromolecules is reflected in the widely diverse scientific specializations participating in the development of ideas in this problem. It is proposed to describe a model of self-duplication consistent with the physical chemistry of the biological macromolecule. In particular, we will consider the fundamental question of the origin of the genetic code via its utility in the self-replication The auto-duplication of an infomation-containing macromolecule (DNA) is considered to be the primary step in the evolution of biological structures. The role of information theory in the kinetics of the process is taken into account. In addition the physical nature of fluctuations will be considered as a primary factor in the origin of the genetic code. A stochastic treatment of the following will be developed

a) Polymerization of a DNA primordial template.

b) Polymerization of a DNA primordial polymerase.

c) Evolution of the protein and DNA via development of the code via random fluctuation in base content.

d) Analysis of the autocatalytic (non-linear) system with consideration of the role of stability on the self optimizing fluctuation process.

e) Evolutionary considerations of the consequences of such a model.

F-PM-C17 A DYNAMICAL MODEL OF PROTEIN FOLDING. David B. Shear, Department of Biochemistry, University of Missouri, Columbia, Mo. 65201

It is often assumed that a globular protein molecule in its native conformation is in a thermodynamically stable state, its free energy being a minimum with respect to variables specifying its shape. By contrast to random coil, flexible polymers, the definite shape revealed by x-ray crystallography suggests that the molecule should be regarded as an elastic solid with a spectrum of oscillatory normal modes. The lowest frequency modes would be the ones most dependent on overall shape, and since for them $h\nu < kT$, they should be fully excited, possess an average energy of kT, and be treatable by classical mechanics. Minimizing the internal partition function yields a result involving the few lowest frequency normal modes as well as the intramolecular potential energy. Spontaneous denaturation suggests that globular proteins may be in a metastable state. The theory allows for a variety of metastable states, which might explain some instances of isoenzymes and some allosteric changes. The theory of normal modes might also be able to explain the unusual complexity, variety and symmetry of snowflakes.

F-PM-D1 MAPPING OF FRAGMENTS OF DNA GENERATED BY RESTRICTION ENDONUCLEASES USING THE DOUBLE-STRAND EXONUCLEASE ACTIVITY OF THE PSEUDOMONAS sp. BAL 31 NUCLEASE. R.J. Legerski‡ J.L. Hodnett‡ and Horace B. Gray, Jr., Department of Biophysical Sciences, University of Houston, Houston, Texas 77004

An extracellular nuclease of Pseudomonas sp. BAL 31 has been shown to degrade linear duplex DNA from the ends in a manner which results in the simultaneous or near-simultaneous shortening of both strands of the DNA at each end. During such degradation, very few internal single-strand scissions are introduced. When duplex DNA which has been partially degraded by the exonuclease activity of the Ps. enzyme is subsequently subjected to the action of a restriction endonuclease and the resulting fragments examined by electrophoresis in agarose-acrylamide composite gels, fragments corresponding to portions of the molecule which have been completely degraded are not present. If a series of such DNA samples, each of which has been subjected to progressively more exonucleolytic digestion, is examined, the order of the various restriction enzyme fragments can be deduced by noting the order in which these fragments at first display an increased migration rate and then become no longer visible. With the aid of this technique, the five fragments produced by digestion of bacteriophage PM2 DNA with the R·Hpa I nuclease have been mapped. Before digestion with the Ps. nuclease and subsequent digestion with the Hpa I endonuclease, the PM2 DNA was converted from its native closed circular duplex form to its linear duplex form with the R·Hpa II enzyme, which cleaves at a single unique site within the circular genome. The R·Hpa II cleavage site has been located with respect to the map of the R·Hpa I nuclease fragments. Experiments in which the technique is extended to more complex fragmentation patterns will be described. Supported by NIH Grant GM-21839 and NIH Postdoctoral Fellowship CA-00695.

F-PM-D2 RESTRICTION ENZYME ANALYSIS OF THE MITOCHONDRIAL DNA FROM CHLAMYDOMONAS REINHARDTII. D. Grant* and K.S. Chiang, Committee on Genetics and Department of Biophysics and Theoretical Biology, The University of Chicago, Chicago, Illinois 60637.

Mitochondrial DNA (mt-DNA) of C. reinhardtii has been analyzed using the restriction endonucleases BamI, SalI, EcoRI, and HindIII, which fragmented the mt-DNA into 2, 2, 4, and 9 fragments, respectively. Using partial and complete digests, the EcoRI fragments were ordered. Double digests (EcoRI-BamI, EcoRI-SalI and BamI-SalI) were used to confirm and extend this fragment map. The above digests, along with those of HindIII-BamI and HindIII-SalI showed conclusively that the 9.9 x 10^6 dalton linear molecules isolated by our procedure possessed unique ends. This result, along with our earlier finding that the mt-DNA can exist in vivo as a supercoiled circular molecule, suggests that the conversion from supercoiled to unit length linear is a site specific process. Control experiments have shown that this circular to linear conversion was not caused by the DNase I treatment of the mitochondria prior to mt-DNA isolation. Mt-DNA isolated from both mating types of C. reinhardtii has been further analyzed with 6 other restriction endonucleases (HaeII, HaeIII, AluI, HincII, HpaII and HhaI), which made 10 or more double-stranded cuts each. No difference in the fragmentation patterns between the mt-DNAs of the two mating types was found. Work is now in progress to test whether mt-DNA from any of the several strains of C. reinhardtii will give different restriction enzyme fragmentation patterns and whether such differences can be used to determine the transmission pattern of parental mt-DNA and its possible correlation with non-Mendelian inheritance in C. reinhardtii. (Supported by USPHS Research Grants, GM 21955 and HD 05804 and USPHS Training Grant GM 00090.)

F-PM-D3 A SYSTEM OF CONSTRAINTS FOR THE RESOLUTION OF SUBCOMPONENTS IN THERMAL DENATURATION PROFILES OF DOUBLE-STRANDED NUCLEIC ACIDS. A. T. Ansevin and D. L. Vizard, Physics Department, The University of Texas System Cancer Center, M. D. Anderson Hospital and Tumor Institute, Houston, Texas 77030

We suggested earlier (Biopolymers 15, 153-174, 1976; Biochemistry 15, 741-750, 1976) that the thermal denaturation of linear, unnicked, naturally occurring DNA occurs in a series of relatively discrete steps, or thermalites. The same assumption is also applicable in large part to the analysis of double-stranded RNA profiles. Our working hypothesis is that a great deal of information about nucleic acid sequence is implicit in accurately recorded high resolution profiles of viral nucleic acids. However, to realize the potential of this method, it is necessary to decompose the observed complex curves into individual thermalites. Because of the high degree of ambiguity involved in such a procedure, it is an easy matter to generate a large variety of "meaningless" resolutions of most profiles. Reducing the degeneracy inherent to a single profile requires a systematic application of constraints, or assumptions about the nature of thermalites. The constraints under study for the analysis of thermal denaturation profiles are: (a) that thermalites should be gaussian in shape with 2σ breadths that are less than $1^{\circ}C$; (b) they should be consistent in number, breadth, and area through a series of profiles on the same DNA at different salt concentrations; (c) the T_m of each thermalite should be a smooth function of the log of the cation concentration of the medium. (Supported by NIH Grant GM 23067)

F-PM-D4 ARRANGEMENT OF INVERTED REPETITIVE SEQUENCES WITH RESPECT TO STRUCTURAL GENES IN HUMAN DNA. Cynthia R. Chuang, Peggy J. Dott*, M. Tien Kuo* and Grady F. Saunders, Dept. of Developmental Therapeutics, The University of Texas System Cancer Center, Houston, Texas 77030.

Inverted repetitive sequences form hairpin-loops in denatured DNA by folding back of a single strand and thus they reassociate with first order kinetics. These sequences have a mean length of 0.2 kb and comprise 6% of the human genome. Since heterogeneous nuclear RNA, the putative precursor of mRNA, contains RNase resistant hairpin structures which are not present in the cytoplasmic mRNA, we investigated the arrangement of inverted sequences with respect to the transcribed genes. Polyadenylated polysomal RNA was isolated from human lymphocytes and transcribed by AMV reverse transcriptase. The resulting ^{3}H cDNA was annealed with (a) unfractionated single stranded DNA fragments of 12 kb and 6 kb, (b) fractions of single strand DNA fragments of corresponding lengths containing inverted repetitive sequences and (c) fractions of corresponding lengths without inverted repetitive sequences. About 65% of the ^{3}H cDNA was driven into duplexes at the maximum Cot value used (10^{4}) following annealing with all DNAs tested. Since the kinetics and extents of reaction were similar in all cases, we conclude that with respect to the total message population the inverted sequences are not an obligatory part of the transcriptional unit. Furthermore, the positions of inverted repetitive sequences are not at fixed locations in the human genome.

F-PM-D5 REPLICATION KINETICS AND DISTRIBUTION OF DNA. W. H. Olson* and M. L. Randolph, Statistics Department, University of Tennessee, Knoxville, TN 37916 and Biology Division, Oak Ridge National Laboratory, Oak Ridge, TN 37830

A mathematical model relating rates of DNA initiation, DNA replication and cell division has been developed for exponentially growing bacterial populations. The derivation comes by analogy with the queuing theory model for a system with random arrivals, constant service time and infinitely many servers. In this analogy arrival, service time and servers correspond respectively to initiation of DNA synthesis, DNA replication time and replication positions. Assuming a symmetric mode of replication, we derive an expression showing that the distribution of replicating positions is Poisson and that they are uniformly distributed along the genome. From this come theoretical expressions in terms of the kinetic parameters for the age (equivalent to length or molecular weight) distribution of DNA and fractional increase of DNA after inhibition of initiation. Using results obtained from bacterial experiments designed to inhibit initiation and yet permit subsequent replication to go to completion we estimate the kinetic parameters. (Research supported by the Energy Research and Development Administration under contract with the Union Carbide Corporation.)

F-PM-D6 DIFFERENCES IN THE REPLICATION OF UNIQUE AND REPEATED NUCLEOTIDE SEQUENCES IN CHO CULTURES. M.R. Mattern and R.B. Painter, Laboratory of Radiobiology, University of California, San Francisco, California 94143

Asynchronous Chinese hamster ovary cultures were prelabelled with ^{14}C-thymidine and then pulse-labelled for different times with ^{3}H-thymidine. Radioactively-labelled DNA was isolated, sheared, and allowed to renature with unlabelled bulk CHO DNA. Nascent DNA from cells given 8 m. pulses renatured with bulk DNA more rapidly than did parental DNA, suggesting that nascent DNA contains a greater than normal percentage of repeated sequences. However, nascent DNA pulse-labelled for 30 or 60 minutes renatured with bulk at the same rate as did parental DNA. DNA from cultures chased for 60 m. following an 8 m. pulse renatured as rapidly as that isolated from cells that were harvested immediately after an 8 m. pulse. In synchronous CHO cultures, DNA synthesised in 8 m. pulses early and late in S-phase contained a greater proportion of repeated sequences than did parental DNA, as judged from renaturation kinetics, whereas that synthesised in an 8 m. pulse in mid S-phase did not. It is concluded that, in CHO cultures, 1) an intrinsic property of the replication of repeated DNA causes its over-representation in DNA labelled with short pulses; 2) a smaller fraction of repeated DNA is replicated in the middle than at the beginning or end of the S period; and 3) there may be different intracellular precursor pools or different rates of DNA polymerisation for the replication of unique and repeated nucleotide sequences.

F-PM-D7 ABERRANT THYMIDINE INCORPORATION IN MUTANTS OF HAEMOPHILUS INFLUENZAE DEFICIENT IN ATP-DEPENDENT NUCLEASE. J.K. Setlow, Biology Department, Brookhaven National Laboratory, Upton, Long Island, New York 11973.

Eight mutants lacking ATP-dependent nuclease and derived by transformation of the wild type by DNA from the originally mutagenized strains exhibit varying degrees of aberrant incorporation of tritiated thymidine. Incorporation starts up more rapidly and shuts off sooner than in the wild type. The degree to which incorporation differs from that of the wild type is correlated with sensitivity to a variety of chemical agents, and the most sensitive mutants with the most aberrant incorporation lack the ATPase activity associated with the ATP-dependent nuclease. An extracellular compound that is dialyzable and impervious to boiling is responsible for most of the aberrant incorporation, in that wild type cells put into medium in which mutants have been growing show a similar aberrant incorporation. The effect of these media can be mimicked by cyclic AMP or cyclic GMP, although there is evidence that neither of these is responsible for the mutants' incorporation kinetics. It is postulated that the mutants are more permeable to many substances than the wild type, partly because of the extracellular compound they excrete. The hypothetical permeability difference is not the result of an alteration in membrane ATPase, since this enzyme in the mutants is indistinguishable from the wild type membrane ATPase. Research carried out at Brookhaven National Laboratory under the auspices of the U. S. Energy Research and Development Administration.

F-PM-D8 REPLICATION OF THE LIPID-CONTAINING BACTERIOPHAGE PR4 IN MEMBRANE MUTANTS OF ESCHERICHIA COLI. D. Auperin*, D. Bzik*, A. Reinhardt*, S. Cadden*, and J. Sands, Department of Physics and Molecular Biology Graduate Program, Lehigh University, Bethlehem, Pennsylvania, 18015.

The lipid-containing bacteriophage PR4 can attach to and replicate in gram negative bacteria that carry one of a group of drug resistance plasmids. Specifically, membrane mutants of *E. coli* can serve as valuable hosts for this phage, and a study of PR4 replication in these mutants might help elucidate the nature of the molecular interactions required for assembly of the virus, specifically at the level of formation of the lipid region of the virion. Use of a glycerol auxotroph as host cell allows determination of the need for lipid synthesis in infected cells. Experiments using this host cell showed that infectious virions are not produced and released if lipid synthesis is stopped earlier than about mid-way through the infectious cycle. Similarly, experiments utilizing a temperature sensitive fatty acid synthesis mutant indicated that a disruption of fatty acid synthesis early in infection significantly reduces the virus yield. Use of a temperature sensitive phosphatidylserine decarboxylase mutant showed that phosphatidylserine to phosphatidylethanolamine conversion could be inhibited as early as about one hour prior to infection without preventing virus replication. These results suggest that overall lipid synthesis is required for phage PR4 replication, but that the level of synthesis of specific phospholipids may be much less important. (Supported by NSF grant PCM 76-12546).

F-PM-D9 ABERRANT DNA INTERMEDIATES IN CELLS INFECTED WITH THE RECOMBINATION DEFICIENT X AND Y MUTANTS OF BACTERIOPHAGE T4. R.J. Melamede, and S.S. Wallace, Department of Microbiology, New York Medical College, Valhalla, New York 10595

At 8 minutes after infection, DNA synthesis, as measured by the incorporation of high specific activity ^{3}H thymidine, is the same in cells infected with $T4^{+}$, T4x or T4y. The DNA intermediates observed at 8 minutes have sedimentation coefficients greater than 1000s as observed on neutral sucrose gradients for wild type- and mutant-infected cells. At 15 minutes after infection, DNA synthesis in T4x- or T4y-infected cells is greatly reduced compared to wild type. At this time, the DNA intermediates formed in mutant-infected cells sediment more slowly than those formed by wild type. The fast sedimenting molecules formed at 8 minutes after infection chase into the more slowly sedimenting forms observed at 15 minutes. The addition of chloramphenicol at 8 minutes after infection allows mutant DNA synthesis at 15 minutes to quantitatively resemble that of wild type. The DNA intermediates observed at 15 minutes in chloromphenicol treated wild type and mutant-infected cells resemble the DNA intermediates formed at 8 minutes after infection.

Supported by PHS Grant CA 12693 from the National Cancer Institute

F-PM-D10 DNA-INDUCED COTTON EFFECTS OF CHEMOTHERAPEUTIC DRUGS AND DYES. Anne K. Krey[1], Department of Molecular Biology, Walter Reed Army Institute of Research, Washington, DC 20012.

Double-stranded calf thymus DNA induced anomalous rotations (Cotton effects) in the optical rotatory dispersion (ORD) spectra of DL-chloroquine, D-chloroquine, DL-quinacrine, methyl green, methylene blue, daunomycin, and distamycin A. None of the drugs and dyes alone exhibited anomalous ORD (Daunomycin not tested). All the induced first Cotton effects were positive. Single-stranded DNA induced anomalies larger than duplex DNA in the ORD spectrum of methylene blue and smaller effects in the spectra of quinacrine and distamycin A. For quinacrine, the effect induced by single-stranded DNA was associated with a different electronic transition than the anomalies produced by double-helical DNA as ascertained by analysis and resynthesis of absorption and optical rotatory dispersion spectra with an analog computer. Such analysis also showed that the anomalies induced by duplex DNA were multiple effects for methyl green, methylene blue, daunomycin and quinacrine but not for chloroquine and distamycin, and that the activities produced by single-stranded DNA were single Cotton effects for quinacrine and distamycin A. For chloroquine, neither single-stranded nor denatured DNA produced anomalous rotations. It is proposed that the Cotton effect induced in the ORD spectrum of chloroquine results from intercalation into DNA and is conformational in origin, while the effects on the ORD spectra of the other substances may involve conformational as well as configurational asymmetric perturbations of chromophores by DNA.

[1]Present address: Department of Microwave Research, Walter Reed Army Institute of Research, Washington, DC 20012.

F-PM-D11 SPIN-LABELED ANALOGS OF 9-AMINOACRIDINE AS PROBES FOR NUCLEIC ACIDS. C.F. Chignell, B.K. Sinha* and V.T. Wee*, Section on Molecular Pharmacology, Pulmonary Branch, National Heart, Lung, and Blood Institute, Bethesda, Md. 20014

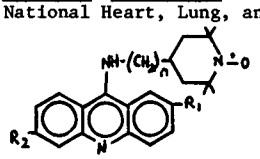

	n	R_1	R_2
I	0	OMe	Cl
II	0	H	H
III	3	H	H

Sedimentation velocity measurements indicated that labels I-III caused unwinding of calf thymus DNA. The T_m value of DNA was increased from 66.5° to 70°, 76° and 73° by I-III respectively. At a concentration of 1 µg/ml, I-III produced a 24%, 56% and 16% inhibition of the growth of leukemia L1210 cells in vitro. At 50 µg/ml, labels II and III inhibited E. coli DNA-dependent RNA polymerase by 23% and 58% respectively, while I stimulated enzyme activity by 20%. The electron spin resonance (ESR) spectra of I bound to DNA, poly dA-poly dT and poly dG-poly dC were characteristic of highly immobilized spin labels with 2 $A_{\parallel}$ values of 59 G, 62.5 G and 57 G respectively. By contrast, the 2 $A_{\parallel}$ values for label II in the same systems were 55.5 G, 55.5 G and 62.5 G respectively. These findings suggest that label II may show some specificity for dA-dT base pairs in DNA. In the presence of DNA, the ESR spectrum of III was characteristic of a nitroxide undergoing rapid motion about its X-axis, indicating that there was little interaction between the piperidine ring and the base pairs. These findings suggest that labels I-III are useful probes for nucleic acids and their biologically important complexes such as histones.

F-PM-D12 CARBON-BOUND AROMATIC PROTONS IN NMR SPECTRA OF TRANSFER RNA. P.G. Schmidt and R.V. Kastrup* School of Chemical Sciences, University of Illinois, Urbana, Ill. 61801

High resolution proton nmr spectra of tRNA in D_2O have generally shown limited resolution in the aromatic region (6.5 to 9 ppm), ostensibly because of the large number (ca. 90) of broad overlapping resonances. But in 220 and 360 MHz spectra of highly purified tRNA we have found that this spectral region actually contains a limited number of very narrow peaks superimposed on a broad background of unresolved resonances. In spectra of valine specific tRNA from E. coli under physiological conditions 25 protons contribute to the narrow signals. Of these, 15 are resolved single proton peaks; most have linewidths (full width at half height) of 4 to 10 Hz. We used the x-ray structure coordinates of phenylalanine tRNA to calculate proton coordinates and with these estimated nmr linewidths of all protons in the macromolecule. A straightforward extrapolation to valine tRNA indicates that all 15 adenosine H-2 protons and 8-10 H-8's of A and G should show narrow lines. Virtually all H-6 doublets of C and U would have broad, unresolvable peaks. The observed spectra bear out these predictions. Heating in D_2O for several hours at temperatures up to 85° led to large reductions in area for some peaks identifying them as H-8 protons which are labile. Changes in temperature, salt concentration, and divalent metal ion concentration are reflected in chemical shift and/or area changes of most peaks. Since these narrow resonances arise from bases in single stranded regions as well as in secondary and tertiary structure, they offer a new, sensitive probe of structure changes throughout tRNA. Supported by NIH Grant GM 18038.

F-PM-D13 PMR STUDIES OF BAKER'S YEAST $tRNA^{phe}$: THE OBSERVED AND THE COMPUTED SHIELDING EFFECTS OF THE METHYL/METHYLENE AND HYDROGEN-BONDED NH RESONANCES. L.S. Kan, P.O.P. Ts'o, M. Sprinzl*, F.v.d. Haar* and F. Cramer*. Div. of Biophys., Johns Hopkins Univ., Baltimore, Md. 21205 and Max Planck Institut Göttingen, W. Germany.

The hydrogen-bonded NH resonances of Baker's yeast $tRNA^{phe}$ in H_2O solution with Mg^{++} have been measured by a 360 MHz spectrometer at 23°C. Fifteen peaks and one shoulder can be resolved which represent 25 ± 1 protons. The methyl and methylene resonances of the same tRNA and its four key fragments in D_2O solution also with Mg^{++} have been measured by both 220 MHz and 360 MHz spectrometers in a temperature range of from 16°C to 98.5°C. A total of 12 methyl and 2 methylene resonances in $tRNA^{phe}$ can be unambiguously assigned. Based on the refined atomic coordinates of the $tRNA^{phe}$ in orthorhombic crystal (A. Rich, private commun.), and on recent advances in the distance dependence of the ring-current magnetic field effects (Giesnner-Prettre et al., Biopolymers 15, 2277 (1976)), a computed shielding (and deshielding) effect of these two kinds of proton resonances was made. The computed chemical shifts are closely similar but not identical to the observed chemical shifts. Interestingly, disagreements for calculated vs. observed spectra all come from the D stem and loop and TψC stem and loop of the $tRNA^{phe}$ molecule. Therefore, the conformation of yeast $tRNA^{phe}$ in aqueous solution is closely similar to that found in the crystal, but is not identical in the TψC and D regions. Recently, Robillard et al.(Nature, 262, 363 (1976)) presented a shielding-effect calculation on the hydrogen-bonded NH proton resonances of the same tRNA molecule. However, their results are considerably different from ours. The differences will be discussed. (Supported by NIH Grant GM 016066 and NSF Grant GB 30725X).

F-PM-D14 DUPLEX FORMATION OF A NONIONIC OLIGODEOXYTHYMIDYLATE ANALOG (d-$[Tp(Et)]_7T$) WITH POLYDEOXYADENYLATE. EVALUATION OF THE ELECTROSTATIC INTERACTION. R. C. Pless* and P. O. P. Ts'o, Division of Biophysics, School of Hygiene and Public Health, The Johns Hopkins University, Baltimore, Maryland 21205.

The heptaethyl ester of heptadeoxythymidylyl (3'-5') deoxythymidine (d-$[Tp(Et)]_7T$ or d-T_8·Et) has been prepared by chemical methods. The material, consisting of a mixture of diastereoisomers, forms a 1:1 complex with $(dA)_n$ in neutral aqueous buffer; this interaction is virtually independent of ionic strength. The octamer triester does not bind to $(dA)_n$·$(dT)_n$, and it interacts with $(rA)_n$ only at low temperatures. By co-chromatography with $(dA)_n$ on Sephadex G-50, d-T_8·Et fractions with different binding affinities for the polyadenylates were obtained. This heterogeneity in binding affinity is ascribed to the diastereoisomerism of d-T_8·Et. Enthalpies of duplex formation were determined by the concentration variation method. At 0.1 M sodium ion concentration, the enthalpy of binding of the various d-T_8·Et fractions to $(dA)_n$ is essentially invariant (-8.1 kcal/mole of base pairs at 0° to -8.6 kcal at 25°) and 1.6 kcal/mole of base pairs more negative than the enthalpy of binding of the phosphodiester analog, d-$(Tp)_7T$, to $(dA)_n$ (-6.8 kcal/mole of base pairs at 11°). This difference is the electrostatic contribution to the enthalpy of duplex formation, arising from the interstrand electrostatic repulsion and the intrastrand repulsion in d-$(Tp)_7T$. The entropy of binding to $(dA)_n$ is more negative for the octamer triesters than for the diester analog, and is different for the various d-T_8·Et fractions. This is interpreted in terms of varying degrees of restriction of rotational freedom for the ethyl substituents upon double helix formation. For the first time, a direct experimental evaluation of the electrostatic interaction of nucleic acid has been achieved. Research supported in part by NIH Grant (GM 016066).

F-PM-D15 BANDING OF POLYTENE CHROMOSOMES BY INDIRECT IMMUNOFLUORESCENCE. P.D. Kurth* and E.N. Moudrianakis, Biology Department, Johns Hopkins University, Baltimore, Md. 21218, and M. Bustin*, Department of Chemical Immunology, Weizmann Institute of Science, Rehovot, Israel (intr. by W.E. Love).

The distribution of the five major histone classes within the polytene chromosomes of the salivary glands of *Chironomous thummi* has been analyzed. Monospecific antisera elicited in rabbits by purified calf thymus histones were combined with the histones in *Chironomous* chromosomes *in situ*, and the resulting complex was stained with fluorescent goat antirabbit IgG. This treatment yielded chromosomes exhibiting characteristic fluorescent banding patterns. The antisera to H2B, H3 and H4 each yielded chromosomal banding patterns that resemble the banding of acetoorcein-stained or phase-contrast-differentiated chromosomes. These three antisera stained the same regions in each of the four chromosomes, a fact which suggests that H2B, H3 and H4 coexist in all the bands. The dense regions, i.e. the bands, stained more intensely than the less compact, interband regions. This suggests that the number of antigenic sites of chromosome-bound histones is proportional to the amount of DNA in a given chromomere. Antibodies to H1 gave a rather diffuse and weak staining, reflecting the limited antigenic cross-reactivity between calf and *Chironomous* H1. Antibodies to H2A also gave weak staining of the chromosomes, which we will demonstrate to be the result of the limited accessibility of the H2A antigenic sites in chromosomes.

F-PM-E1 STRUCTURE OF 1-METHYLTHYMINE DIMERS PRODUCED BY MONOCHROMATIC (254 nm) AND SOLAR IRRADIATION. P. Martel* and B.M. Powell* (Intr. by M.C. Paterson), Atomic Energy of Canada Ltd., Chalk River, Ontario, Canada, K0J 1J0.

As a preliminary to determining the detailed molecular configurations involved in the photodimerization of various pyrimidine structures, including those in DNA, structural changes resulting from irradiation with 254 nm ultraviolet light have been observed in polycrystalline 1-methylthymine by the technique of neutron diffraction. The dose rate for the irradiations was ~10^{16} photons/cm^2-s. Shifts and intensity changes of the powder diffraction peaks have been measured as a function of the irradiation time, and the crystal lattice parameters were found to vary linearly with the concentration of dimers formed. The changes are interpreted as the formation of photon-induced dimers between adjacent molecules. The adjacent molecules are bound together to form the photodimer by a rectangular cyclobutane ring of dimensions 0.14 nm by 0.19 nm. Our best fit to the data suggests that the molecules tilt about their centres of gravity by ~44° in order to form dimers. The molecules are also distorted with some of the intramolecular bonds and bond angles changing by as much as 0.016 nm and 8.1 degrees respectively. These distortions are a measure of the minimal forces involved in the dimerization process. Polychromatic irradiation was also carried out using natural sunlight received through a cloudless sky over a 3¼h period about noon at Chalk River (~46° latitude, ~140 m above sea level), on August 5th, 1976. A similar amount of damage (~13% dimer concentration) resulted for roughly the same exposure time involved in the monochromatic exposures. Some of the separations and intensities of the peaks are slightly different for the two kinds of irradiation, but there is a general similarity of the diffraction patterns as a whole which indicates that the nature of the damage is similar for either solar or 254 nm radiation.

F-PM-E2 ELECTRORETINOGRAPHIC AND FUNDUSCOPIC CHANGES INDUCED BY HEAVY CHARGED PARTICLE IRRADIATION OF CATS EYES. C.T. Gaffey and V.J. Montoya*, Lawrence Berkeley Laboratory, University of California, Berkeley, CA 94720

The Bevalac at the Lawrence Berkeley Laboratory generates an 8 GeV neon ion, pulsed beam. Pulses occur at 15/minute with a peak intensity of 2 x 10^9ions/pulse. In ocular exposures circular beams (38 mm diameter) were obtained by absorption collimators. Dose rates of 140 to 474 rad/minute were measured with parallel ionization chambers. The accelerated neon ions used in cat exposures have an energy of 400 MeV/nucleon, a charge of +10, and a range of 14 cm in water. Heavy particle irradiations in these experiments were restricted to the plateau region of the beam; the linear energy transfer was 32 keV/micron of water for this section of the charged, ion beam. The susceptibility of the electroretinogram (ERG) of the dark adapted eye to particle damage was studied as a function of the absorbed neon ion dose and the postirradiation time. The neon particle dose to completely inhibit the cat's ERG was established. Similarly, the amounts of 200 Kv X-rays required to fully suppress the a- and b-wave amplitude of the ERG were determined. This approach permitted the relative biological effectiveness (RBE) to be estimated. It was our finding that the RBE for neons to compromise vision was approximately three compared to a standard value of one for X-rays. When two flashes are presented to a cat's eye, each photic stimulus evokes an ERG. As the interflash interval (IFI) is shortened, the retina generates an attenuated response to the second flash. IFI studies demonstrate that the recovery state of the retina is remarkably depressed by irradiation. Normal fundus photography, fluorescien angiography and retinal sections for light microscopy were used to suggest a mechanism of irradiation injury. This work was performed under the auspices of the National Aeronautic and Space Administration.

F-PM-E3 **A NEW ENZYMIC PHENOMENOLOGY: ENZYME REACTION WITH IRRADIATED SUBSTRATES.** **S.Comorosan, Department of Biochemistry, Postgraduate Medical School, Fundeni Hospital, Bucharest, Romania.**

Enzyme reaction rates are enhanced when the corresponding substrates are irradiated in crystalline state with visible light. We have termed the physical modification induced in the substrates through this particular technique the S⟶S* transition. This new type of transition raises basic physical as well as biological questions. The majority of the substrates used in these experiments do not absorb in the 546 nm domain. The capability of S*-substrate to enhance the enzyme reaction rate after its dissolvation lasts up to 2 hours. This unexpected long lifetime in solution, resisting the energy-dissipating effects of thermal motion, is certainly unusual in physics. New concepts may be required to explain the physics of this phenomenon. We have investigated with irradiated substrates a series of enzymes comprising a well determined metabolic sequence, extracted from a single biological source. The substrate irradiation times that enhanced the respective reaction rates proved to be similar for the whole series of enzymes in the metabolic pathway. This may suggest the concept of a "metabolic flux" which could modulate long metabolic sequences, in the context of a new type of cellular control mechanism. Likewise, the S⟶S* transition "seen" by the enzyme may suggest a series of conjectures concerning the discriminating power of biological molecules as well as a possible submolecular basis for the biological specificity.

F-PM-E4 **DEPENDENCE OF SUBSTRATE IRRADIATION ACTIVATION CHARACTERISTICS ON ENZYME SOURCE.** George E.Bass* (Intr. by D.J. Marsh), Dept. Mol. Biol., College of Pharmacy, University of Tennessee, Memphis, TN.38163.

Comorosan et al.have reported that the particular values of the characteristic parameters for several enzyme/substrate reactions investigated in the context of reaction rate enhancement by pre-irradiation of crystalline substrate may depend on the species from which the enzyme is isolated. Our studies reported here confirm and extend this finding. The characteristic parameters for this phenomenon are t_m, the minimum substrate irradiation time which leads to enzyme reaction rate enhancement, and τ, the constant increment of irradiation time separating subsequent rate enhancements. The Comorosan group has found the yeast LDH/pyruvate reaction rate enhanced for t_m = 5 sec, τ = 30 sec, and the yeast LDH/lactate reaction rate enhanced for t_m = 20 sec, τ = 30 sec. The corresponding values for rabbit muscle LDH were, for the pyruvate reaction, t_m = 5 sec, τ = 30 sec, and for lactate reaction, t_m = 15 sec, τ = 30 sec. We have investigated and found identical values of these parameters for the pyruvate and lactate reactions with LDH isolated from rabbit muscle, beef heart and human erythrocytes as well as the M4 and H4 isozymes. On the other hand we have found different parameter values for chicken heart LDH, specifically, t_m = 15 sec, τ = 20 sec, for pyruvate and t_m = 5 sec, τ = 15 sec for lactate. Thus, we confirm identical values for the several mammalian sources investigated and further, an alteration in parameters values on going to a non-mammalian source.

F-PM-E5 DNA TURNOVER IN BUFFER-HELD ESCHERICHIA COLI AND ITS EFFECT ON REPAIR OF UV DAMAGE. M. S. Tang*, V. T. Wang*, and M.H. Patrick, The University of Texas at Dallas, Programs in Biology, Box 688, Richardson, Texas 75080.

Continuous DNA degradation and resynthesis, without a net change in cellular DNA content, were observed in buffer-held, unirradiated E. coli B/r. The amount of DNA degradation is not influenced by prior exposure to UV radiation, but the synthetic activity of buffer-held cells, which appears to be carried out primarily by DNA polymerase I and to lead to restoration of the intact genome, is inversely correlated with the UV fluence. The average size of newly synthesized DNA is estimated to be at least 150 nucleotides per patch. We suggest that this DNA turnover can result in "nonrepair sites" in the DNA of a UV-irradiated cell when the degradation occurs opposite to a cyclobutyl dipyrimidine. This implies that both beneficial (excision repair) and deleterious processes (DNA turnover) take place in buffer-held cells, and that cell survival depends on the delicate balance between DNA turnover and repair. Based on these findings, we propose a model to explain the limited repair observed during post-irradiation liquid-holding and to account for the large difference in cell survival between irradiation at low fluence rates and at high fluence rates followed by liquid-holding.

F-PM-E6 EVIDENCE FOR TWO MODES OF DNA DEGRADATION IN E. COLI FOLLOWING UV IRRADIATION. K. Fong and R.C. Bockrath, Department of Microbiology, Indiana University School of Medicine, Indpls., IN 46202

UV-induced DNA degradation has been found in wild-type E. coli strains but not in strains deficient in the endonucleolytic step of excision repair for pyrimidine dimers (uvrA mutants). DNA degradation in wild-type cells is greatly reduced by photoreactivation. This suggests that DNA degradation is initiated at pyrimidine dimers. We also find post-UV incubation in the presence of chloramphenicol to cause significant DNA degradation in a uvrA strain. The extent of this degradation is not reduced by photoreactivation, implying that chloramphenicol-enhanced degradation represents a second mode of DNA degradation.

We find greater DNA degradation in wild-type cells irradiated at -79° C than in cells irradiated at ambient temperature (21° C). When the cells are irradiated at 21° C the amount of degradation is markedly decreased by photoreactivation, whereas the amount of DNA degradation in cells irradiated at -79° C is only slightly decreased by photoreactivation. This suggests that at -79° C the major UV lesions leading to DNA degradation are not pyrimidine dimers, but probably DNA-protein cross-links which are known to be produced in large amounts at -79° C. Supported by N.I.H. grant GM 21788.

F-PM-E7 MOLECULAR MECHANISM OF PHOTOOXIDATION IN CELLS. Joan E. Roberts and Arthur Grollman,* Department of Pharmacology, SUNY at Stony Brook, Stony Brook, N.Y. 11790

Irradiation of a biological substrate (DNA,protein,RNA) in the presence of certain dyes and drugs and in the presence of oxygen produces a photosensitized oxidation of the substrate. There are at least two mechanisms by which the reaction can proceed. The sensitizer, excited to the triplet state, can react either directly with the substrate via a redox mechanism involving free radicals (TYPE I) or with oxygen via a singlet oxygen intermediate (TYPE II). Differentiation of these mechanisms using a variety of organic or isolated biological substrates and sensitizers has been previously reported. A system has been developed to study the mechanism of photooxidation in cells, adapting techniques and equipment formerly used for photochemical experiments. Non-toxic free radical and singlet oxygen quenchers were added to cells and sensitizer before controlled irradiation to interrupt the formation of the appropriate excited state intermediate. The molecular mechanism of photooxidation for the system was then deduced by examining the extent of photooxidative damage in the presence and absence of quenchers. Specifically, the photooxidative damage (inhibition of DNA synthesis) to HeLa cells by proflavin irradiated with visible light (400-450nm) under physiological conditions was drastically reduced in the presence of free radical quenchers (glutathione, penicillamine) and not significantly affected by the presence of singlet oxygen quenchers (α-tocopherol, β-carotene, DABCO). This indicated the molecular mechanism for this system is most probably TYPE I. The same methodology would be appropriate in the study of other sensitizers with cells. Toxicity studies of the above mentioned and other quenchers (BHT, hydroquinone) will be included.

F-PM-E8 GROUND AND EXCITED STATE INTERACTIONS BETWEEN PROFLAVINE AND NUCLEOTIDES. M. G. Badea* and S. Georghiou, Department of Physics, University of Tennessee, Knoxville, TN. 37916

The interaction between the mutagenic acridine drug proflavine and the nucleotides GMP, CMP, AMP, and TMP in aqueous solution has been investigated by spectrophotometric, spectrofluorometric and nanosecond fluorometric techniques. Molecular complex formation between ground state as well as excited state proflavine and all four nucleotides has been observed. For the proflavine-GMP complex the stoichiometry has been shown to be 1:1. Its association constant has been found to increase from 310 M^{-1}, when proflavine is in its ground electronic state, to 1550 M^{-1}, when proflavine is in its first excited singlet state. Thus, light absorbed by the mutagenic drug alters its reactivity, which, in turn, results in an appreciable increase in its ability to bind to the nucleotide. The implications of these findings concerning the proflavine-DNA interaction as well as the possible importance of electronic excitation in acridine mutagenesis will be discussed. A structure of the complex will be proposed involving hydrogen bond formation between reactive groups of proflavine and of GMP.

F-PM-E9 SEARCH FOR AN INDUCIBLE SYSTEM RESPONSIBLE FOR MUTAGENESIS IN MAMMALIAN CELLS. J.E. Cleaver, Laboratory of Radiobiology, University of California, San Francisco, California 94143

Inducible repair systems which are responsible for error-prone repair and mutagenesis have been clearly identified in prokaryotic cells but not in eukaryotic cells. Unfortunately, the concept of inducibility may often merely provide an easy way to explain complex data without thereby becoming a proven phenomenon. It is essential therefore to employ experimental approaches that are capable of demonstrating the absence as well as presence of inducible repair. One way this can be done is if the lesions presumed to induce a hypothetical error-prone repair process are distinct from those to be repaired erroneously. Since X rays do not produce ouabain resistant (O^R) mutations in CHO cells, but UV light does, it is possible to use X rays as a repair inducer that is non-mutagenic and then determine the subsequent yield of UV-induced O^R mutants. X rays (100 to 400 r) given before UV (7.8 to 13 J/m^2) have no effect until the interval between irradiation exceeds 4 hr, whereupon there is an increase of 30 to 40% in yields of O^R mutants, but no change in 6-thioguanine (TG^R) resistant mutants. Since O^R mutations are probably point mutations whereas TG^R mutations are of all kinds, with probably a minority point mutations, the results indicate that if an inducible error-prone system exists in CHO cells it is (a) induced slowly by X rays, (b) has a small influence in overall mutant yields, and (c) affects point mutation frequencies but not deletion frequencies. Within the accuracy afforded by these experiments, however, there is little evidence for a major role of inducible repair systems over short time intervals in mammalian mutagenesis. Work supported by U.S. Energy, Research, and Development Administration.

F-PM-E10 SOME BIOPHYSICAL STUDIES WITH CHINESE HAMSTER CELLS IRRADIATED WITH ENERGETIC HEAVY ION BEAMS. J. D. Chapman, Medical Biophysics Branch, Atomic Energy of Canada Ltd., Pinawa, Manitoba, ROE 1LO and E. A. Blakely*, K. C. Smith*, and C. A. Tobias, Biomedical Division, Lawrence Berkeley Laboratory, University of California, Berkeley, CA 94720.

DMSO, previously shown to be an efficient scavenger of OH in mammalian cells, was found to protect G_1-phase Chinese hamster cells against the lethal action of energetic He, C, and Ne beams. This result suggests that the chemistry of indirect action contributing to cell inactivation by X-rays or by these particle beams is not qualitatively different. The radioprotective effectiveness of DMSO was greatly reduced and was qualitatively different for cell inactivation resulting from energetic Ar ions.

The radiation biological effectiveness (RBE) of the He, C, Ne, and Ar beams was studied with homogeneous populations of mitotic, G_1-phase, and stationary phase cells. Ultrastructural and radiobiological differences were known to exist between these phases of cell growth. At a linear energy transfer (LET) of 100-150 Kev/μ, which produced the maximum RBE observed, all cell types had similar values of single-hit inactivation. At lower LETs their radiosensitivities were different and for 220 kVp X-rays or energetic He ions the relative single-hit radiosensitivities of stationary phase, G_1-phase, and mitotic cells were 1, 2, and 8, respectively. These studies emphasize the fact that numerical values of RBE are strongly dependent upon the effectiveness of the standard radiation used and this, in turn, can depend upon the state of growth of the cell system studied. Presumably different conformations of the cell's molecular targets are responsible for the wide difference in effectiveness of the low LET radiations.

F-PM-E11 MECHANISM OF ACTION OF α-PARTICLES ON NUCLEIC ACID COMPONENTS: AN ESR STUDY. L.S. Myers, Jr., R.B. Ingalls*, and S. Alkaitis*, Laboratory of Nuclear Medicine and Radiation Biology, and the Department of Radiological Sciences, University of California, Los Angeles, California 90024

A technique has been developed for using cyclotron accelerated 24 MeV helium ions to simulate effects of α-particle radiation on nucleic acid and its components. In the first studies, trapped radicals formed by exposure of thymidine and other nucleosides were investigated by ESR spectroscopy. The technique consists of reducing the energy of the helium ions to about 11 MeV by passing the beam through metal foils. (This energy is within the range of energies of α-particles emitted by transuranic elements by radioactive decay.) The particles impinge on the compound of interest in an evacuated system cooled by liquid nitrogen. After exposure the samples are transferred to an ESR sample tube, and measured at room temperature. Spectra of radicals in irradiated thymidine are almost identical with spectra of radicals produced by low LET radiation. The principle radical is the 5,6-dihydrothymidin-5-yl radical.Exposure of the radicals to air causes little if any change in the spectra, indicating that neither oxygen nor water can diffuse to the radical sites. Studies will be continued with other nucleosides and DNA, attempts will be made to carry out the entire experiment at liquid N_2 temperature, and product analyses will be carried out to determine whether the product and ratios of yields of trapped radicals to total damage for α-radiation differ from those for low LET radiation. Work was done in cooperation with the UCLA Biomedical Cyclotron Facility. (Supported by the U.S. Energy Research and Development Administration)

F-PM-E12 PHOTOLYSIS OF (ISO)DESMOSINE, DIHYDRODESMOSINE AND ELASTINE. F. Lamy, R. Baurain*, M. Guay* and J.F. Larochelle*. Department of Biochemistry, Sherbrooke University, School of Medicine, Sherbrooke, P.Q. J1H 5N4, Canada.

It is known that the pyridinium ring of a model compound such as N-methyl pyridinium chloride is cleaved by U.V. radiation at 254nm. At acid pH the product obtained are methylamine and glutaconaldehyde. Under the same conditions desmosine and isodesmosine are degraded into lysine and probably into the homologous substituted cetone of glutaconaldehyde. At pH 6.0 - 7.0, a transient open-chain aminoaldehyde intermediate is observed which can either reform the original compound or be cleaved as at low pH. When intact elastin is photolysed for 20 minutes in water, approximately 75% of the (iso)desmosines are destroyed, accompanied by an increase of free lysine residues. No change in the concentration of the other amino acids, including tyrosine, are noted. It is therefore likely that the cross-links engaged in peptide links are also cleaved photochemically. As a model for the dihydroisodesmosine, 1,2-dipropyl-3,5-diethyl-1,2-dihydropyridine has been synthesised and photolysed at 330nm. As in the case of the aromatic compounds, the bonds around the nitrogens are broken. Propylamine and a open-chain aldehyde is obtained.

F-PM-F1 DETERMINATION OF DNA MOLECULAR WEIGHT BY VISCOELASTIC MEASUREMENTS. B.C. Bowen and B.H. Zimm, Department of Chemistry, University of California, San Diego, La Jolla, Ca. 92093.

The viscoelastic properties of bacteriophage T2 DNA solutions have been used to determine the NaDNA molecular weight in four independent ways from the theory of the beads-springs model. The four molecular weights were 132.9, 132.1, 131.7 and 128.6 x 10^6. Creep-recovery recoil curves were measured upon the cessation of steady-state shearing of dilute solutions. The measured properties were: A (time integral of the recoil curve), Γ (total recoil amplitude), Γ_{11} and τ_{11} (recoil amplitude and retardation time, respectively, of the slowest relaxing component), and η_{sp} (specific viscosity). Each of these quantities depended on DNA concentration c and the steady-state shear rate κ; it was necessary to extrapolate to zero values of each. The shear rate dependence could be expressed in terms of a dimensionless parameter $\kappa\tau_{11}$. (For example, at c = 7.17 µg/ml and $\kappa\tau_{11}$ = .21, the apparent molecular weight calculated from τ_{11} and Γ_{11}, $M_{\tau\Gamma 11}$, was 134.7 x 10^6. At the same concentration and $\kappa\tau_{11}$ = 1.80, $M_{\tau\Gamma 11}$ = 219.1 x 10^6.) The four molecular weights were $M_{\tau\eta}$, $M_{\tau\Gamma 11}$, $M_{\tau\Gamma}$, $M_{\tau A}$, each different in its sensitivity to molecular weight distribution. Their agreement suggests (1) that the theoretical equations relating each M to the corresponding measured quantities are valid, and (2) that the solutions were nearly homogeneous in intact T2 DNA molecules. These M's represent maximum molecular weights because the presence of a small amount of highly fragmented DNA (shown by electron microscopy to be less than 5% by weight) would reduce the actual concentration of intact molecules, to which each M is proportional.

F-PM-F2 IS ROTOR SPEED DEPENDENCE OF DNA SEDIMENTATION RATE A TUBE WALL EFFECT AND THUS AVOIDABLE UNDER PROPER CENTRIFUGATION CONDITIONS? C.S. Lange and R.W. Clark*, Departments of Radiology, Radiation Biology & Biophysics, University of Rochester School of Medicine and Dentistry, Rochester, New York, 14642.

The Zimm model [1] explaining rotor speed dependence has become widely accepted as a valid description of DNA sedimentation in high g force fields. This is surprizing since the model has not yet been quantitatively verified. Furthermore, there are difficulties with the evidence providing only qualitative support. This support has come from several laboratories where an (RPM)^4 or an M^4(RPM)$^4R^2$ dependence has been found using swinging bucket rotors. Rubenstein & Leighton [2] also noted "...that the nature of the centrifuge tube [nitrocellulose vs. polyallomer] influences the sedimentation coefficient of T2 DNA is completely unexpected and unexplained." and concluded that "...high rotor speeds...must be affecting [the DNA's] frictional coefficient.". These ignored and unconnected observations led us to postulate [3] that the friction of interest is that between the DNA and the tube wall rather than DNA and the solvent. If this postulate is correct, then zonal rotors should not show any rotor speed dependence. Two observations indicate this to be the case. (1) Wheeler et al. [4] showed that 16S single stranded DNA sediments with the predicted (RPM)$^4R^2$ dependence in two swinging bucket rotors but found no such dependence in two zonal rotors, contrary to expectation. (2) We [3] demonstrated the absence of rotor speed dependence for native linear B. subtilis DNA (2x10^7) in the Ti-15 zonal rotor. Data and the model will be discussed to demonstrate that ignoring data which don't fit preconceived views leads to erroneous conclusions. Work performed under ERDA contracts (Nos. AT(11-1)3501 & 3490) UR-3490-1016, & NCI/RCDA # 5K04CA70299. [1 = Biophys. Chem., 1, 279 (1974); 2 = ibid., 292; 3 = Biophys. J., 16, 145a (1976), Biopolymers, 16, (1977,in press); 4 = Anal. Biochem., 64, 329 (1975)]

F-PM-F3 FRICTIONAL PROPERTIES OF BACTERIOPHAGE T7 DNA IN PRESENCE OF METHYLMERCURIC HYDROXIDE CH_3HgOH. D. W. Gruenwedel and S. E. Brown*, Department of Food Science and Technology, University of California, Davis, California 95616

The effects of increasing concentrations of CH_3HgOH on the rate of sedimentation, S°, (the superscript ° indicates vanishing polymer concentration) and intrinsic viscosity, [η], of T7 DNA were studied at 20° and at pH 9.18 (0.005 M Na-borate) in 0.005, 0.05, and 0.5 M Na_2SO_4, respectively. Both S° and [η] are independent of organomercurial concentration as long as DNA remains native. Denaturation, brought about by complexing of CH_3HgOH with the polymer, produces large changes in S° and [η]. The frictional coefficient of T7 DNA, defined as $f_2^\circ = M_2(\partial\rho/\partial c_2)_\mu^\circ/S^\circ\eta_r N_A$, where M_2 is the molecular weight of T7 DNA, c_2 its concentration in grams per milliliter of solution, $(\partial\rho/\partial c_2)_\mu^\circ$ the "buoyancy factor" of the four-component system under study (the subscript μ indicates constancy in the chemical potentials), and where η_r and N_A are, respectively, the relative viscosity of the salt medium and Avogadro's number, was evaluated for all three salt solvents as a function of organomercurial concentration. f_2° of native T7 DNA was found not to be sensitive to changes in ionic strength or organomercurial concentration. f_2° of single-stranded and methylmercurated T7 DNA varied strongly with salt concentration. However, since, at a given salt concentration, f_2° of denatured T7 DNA was barely affected by CH_3HgOH it is concluded that the dramatic variations of S° with organomercurial concentration, observed in the post-denaturation region, reflect only changes in the (thermodynamic) "preferential solvation" of T7 DNA but not changes in its three-dimensional conformation. Research supported by USPH GM 16282.

F-PM-F4 DIFFUSION COEFFICIENTS AND STRUCTURAL PROPERTIES OF THE fd BACTERIAL VIRUS[1]. J. Newman‡[2] H. L. Swinney‡ and L. A. Day, (Intr. by F. C. Chen) Physics Department, City College, New York, N.Y. 10031 and Public Health Research Institute of New York, N.Y. 10016

An improved transient electric birefringence technique[3] was used to measure the rotational diffusion coefficient D_R of the rod-shaped fd bacterial virus as a function of concentration (0.5 - 1000 μg cm^{-3}) and ionic strength (1 and 12 mM). The use of a low-powered laser, crystal polarizing optics, and signal averaging made possible measurements of high accuracy (~ 1% std. dev.) with very low electric fields (10 - 360 V cm^{-1}), even at low concentrations (~ 1 μg cm^{-3}). The low concentration result, $D_R^{20} = 20.9 \pm 0.3$ sec^{-1}, allows us to calculate a virus length of 9150 ± 120 Å from the Broersma equation for D_R. (All uncertainties here are quoted at the 95% confidence limit.) Small angle intensity fluctuation spectroscopy was used to measure the translational diffusion coefficient D_T of the fd with the result $D_T^{25} = (2.56 \pm 0.06) \times 10^{-8}$ $cm^2 sec^{-1}$. This result is, within experimental error, in agreement with the value calculated from the Broersma equation for D_T for a 9150 Å rod. From these results and previously determined chemical composition, sedimentation velocity, and density increment data for fd under the same sample conditions, we obtain values for the molecular weight of the virus and its DNA and for the protein subunit and nucleotide average axial spacings.

[1]Research supported in part by a grant from The City University of New York and in part by a grant from the U.S.P.H.S.
[2]Present address: Biophysics Department, Johns Hopkins University
[3] J. Newman and H. L. Swinney, Biopolymers 15, 301-315 (1976)

F-PM-F5 IMPLICATIONS OF PHYSICAL PARAMETER CHANGES WHICH OCCUR UPON FOLDING THE 30S RIBOSOMAL SUBUNIT. Walter E. Hill* and Donald P. Blair, Department of Chemistry, University of Montana, Missoula, Montana 59812

It has been previously shown that ribosomal subunits can be loosened or unfolded by decreasing the magnesium concentration of the particles. By carefully monitoring the change in the sedimentation coefficients, diffusion coefficients and density increments of the unfolded 30S ribosomal subunits under various ionic conditions, it has now been shown that a decrease in sedimentation coefficient is not necessarily due to a structural loosening of the macromolecule. Conversely, a structural loosening of the macromolecule can take place without the sedimentation coefficient being appreciably affected. Results on the unfolded stages of the 30S ribosomal subunit show changes in all three of the above mentioned physical parameters, as well as molecular weight changes which occur. The implications of these results on measured physical characteristics of macromolecules will be discussed.

This work was supported in part by NIH research grant #GM17436 and Career Development Award #GM19692 (WEH).

F-PM-F6 EQUILIBRIUM SEDIMENTATION MEASUREMENTS ON THE DISK-SIZED INTERMEDIATE OF TOBACCO MOSAIC VIRUS PROTEIN. C. L. Stevens and S. Loga,* Department of Life Sciences, University of Pittsburgh, Pittsburgh, PA 15260.

The polymerization in vitro of tobacco mosaic virus protein involves a sequence of reactions beginning with the monomer (17,500 MW) and ending with the virus-like rod (40 x 10^6 MW). For instance, the first reaction is a trimerization which occurs without proton binding. Fortunately, using equilibrium centrifugation, some of these reactions can be observed without interference from others. There appears to be two modes of assembly of trimers. When pH is relatively high (0.1 μ phosphate buffer, pH 6.8, 15°C), we observe that trimers associate by condensation (indefinite) polymerization. This is in agreement with findings of others. When pH is lowered to 6.5 and temperature to 11°, other conditions being the same, we observe only trimers in equilibrium with a species of about 33 subunits. This size is equivalent to the double disk or the two-turn helix. We are unable to detect species intermediate to 3 and 33 subunits. (Intermediates consisting of no more than a total of about 10% of the mass of protein would probably go undetected, especially if the degree of polymerization was low). It is likely that the pH drop has promoted the formation of the 33 subunit aggregate; on the other hand, it has not promoted the condensation process. Indeed, the condensation polymers largely disappear, but the trimer level remains. The data suggest that trimers assemble themselves in one of two parallel pathways, condensation or formation of the disk-sized aggregate. (This work was supported by NIH grants GM 10403 and GM 22558).

F-PM-F7 RHEOLOGY OF DEFORMABLE AND NONDEFORMABLE ERYTHROCYTE SYSTEMS AGGREGATED BY DEXTRAN T-70. G.V.F. Seaman, R.J. Knox, F.J. Nordt and D.E. Brooks, Department of Neurology, University of Oregon Health Sciences Center, Portland, Oregon 97201.

Dextrans (Dx) in excess of 40,000 MW can induce weak cell aggregation of native human erythrocytes (RBC) and formaldehyde-fixed RBC (F-RBC) by macromolecular bridging. Cell aggregation measured both microscopically and by a low shear rheological method published previously increases to a maximum at a characteristic Dx concentration ([Dx]) and then diminishes at higher [Dx]'s and is absent above a characteristic [Dx]. Elevation of bulk [Dx] through this range gives proportional increases in adsorbed polymer and is accompanied by increases in the electrophoretically measured zeta potential (ζ) of the cells. The correlation of the ζ's at disaggregation and the low shear behavior of RBC in the presence of Dx support the notion that intercellular electrostatic interactions are an important opposing force to polymer bridging and that weak aggregation could be detected by low shear viscometry. To establish the role of cell deformation in the rheological estimation of aggregation, the degree of aggregation, ζ's, and behavior at low shear were compared for deformable RBC and nondeformable F-RBC in media of differing ionic strengths and [Dx]'s. In contrast to RBC, F-RBC aggregated weakly at [Dx]=0 at ionic strengths > 0.03 M and higher [Dx]'s were required to disaggregate the cells. The ζ's at ionic strengths at the disaggregation point of F-RBC at high [Dx]'s were approximately constant but were consistently higher than for RBC. The rheological estimation of aggregation provided a satisfactory index of the extent of cell-cell adhesion for RBC, but it gave no indication of very weak aggregation of F-RBC under the measurement conditions employed. Supported by the National Institutes of Health, Research Grant HL 15855.

F-PM-F8 FLOW BIREFRINGENCE CHANGES IN HYALURONATE SOLUTIONS AS A FUNCTION OF SOLUTION PH. T.W. Barrett and R.E. Harrington, Department of Physiology & Biophysics, University of Tennessee Center for the Health Sciences, Memphis, TN 38163 and Department of Chemistry, University of Nevada, Reno, Nevada 89507.

The molecular dynamics of hyaluronate solutions have reference to the function of many physiological systems[1]. It is possible that optimum functioning of such systems is dependent upon the maintenance of system pH within certain limits. In order to investigate this possibility the flow birefringence of hyaluronate solutions of varying pH were investigated using a low velocity gradient apparatus[2]. The data obtained at different hyaluronate concentrations (0.25-0.0625%) demonstrate a large change in optical anisotropy as a function of pH, with most of the transition in the pH range 7.0 to 7.5, i.e., across the physiological range. The sign of the anisotropy changes between pH 8.0 and 8.5. This result, together with changes in the extinction angle and intrinsic viscosity as a function of pH, suggest a pH-dependent structural change in the system.

[1]Barrett, T.W. Biochimica et Biophysica Acta 385 (1975) 157; Physiological Chem. & Physics, in press.
[2]Harrington, R.E. Biopolymers 9 (1970) 141.

This research was supported by an Alfred P. Sloan Foundation grant (Southern Regional Education Board).

F-PM-F9 CONFORMATIONAL CHANGES OF HYALURONIC ACID IN ETHANOL-WATER SOLVENT. J. W. Park* and B. Chakrabarti, Department of Retina Research, Eye Research Institute of Retina Foundation, 20 Staniford Street, Boston, Mass. 02114

Hyaluronic acid shows marked circular dichroism(CD) and optical rotatory dispersion(ORD) changes upon addition of ethyl alcohol in the acidic solution forming a gel-like state. The changes include blue shifts of ca 210 nm negative CD band and ca 220 nm ORD trough by more than 20 nm, and appearance of a positive CD band near 226 nm revealing the negative CD band ca 242 nm. The pH and ethanol concentration dependences of these variations were studied. Viscosities of hyaluronic acid in water and 10% ethanol-90% water solvents both at pH 2.6 were studied in the temperature range of 15-60°. Sharp transition in viscosities (η, η_{rel}, $[\eta]$) was observed in the 10% ethanol solvent at 40-50°, but no such transition was observed in the water solvent. For example, intrinsic viscosity of hyaluronic acis in the 10% ethanol solvent is ~2.8 times higher than that in the water solvent at 25°. At 50°, little difference in the intrinsic viscosities of hyaluronic acid in both solvents were observed.

F-PM-F10 VACUUM ULTRAVIOLET CIRCULAR DICHROISM OF POLYSACCHARIDES. E. S. Pysh, Department of Chemistry, Brown University, Providence, R.I. 02912

Polysaccharides consistently display two optically active transitions in the vacuum uv, one near 180 nm and the other near 160 nm. The 180 nm band is positive in several galactomannans and in agarose, and negative in ι-carrageenan. The 160 nm band is of opposite sign in those polymers.

In ι-carrageenan the CD changes during the helix-coil transition. In galactomannans the intensity of the 180 nm band changes as a function of the galactose/mannose ratio.

In hyaluronic acid the amide and carboxyl transitions dominate the CD. The amide $\pi-\pi^*$ transition of the N-acetyl glucosamine moiety is strongly optically active in the solid state helical structure, but weakly active in solution.

The sol-gel transition in agarose can be followed using the 180 nm transition. With a high temperature vacuum uv cell, the 180 nm CD band can be observed in both gel and solution forms at the same temperature.

These results indicate that the vacuum uv CD of polysaccharides reflects characteristics of both primary and secondary structure.

F-PM-F11 ORIENTATION OF ACTIN AND MYOSIN FILAMENTS IN INTERMEDIATE STRENGTH MAGNETIC FIELDS T. William Houk and T.A. Smith*; Dept. of Physics, Miami University, Oxford, Ohio 45056.

A number of investigations have indicated that muscle tissue has sufficient diamagnetic susceptibility to be oriented by relatively weak static magnetic fields (Faraday, M., 1855, Exp. Res. Elect., London. 3, 27; Arnold, W., et al., 1958, Proc. Nat. Acad. Sci., USA, 44, 1). Such orientation is also exhibited by rod outer segments and appears to be due to the regular arrangement of molecules within the disk membrane (Chalazonitis, N., et al., 1970, Comp. rend. 271, 130; Hong, F., et al., 1971, Proc. Nat. Acad. Sci. USA, 68, 1283). We have investigated the possibility that, due to their structure, thin and thick filaments may individually possess sufficient susceptibility to be aligned by magnetic fields in solution. Changes in orientation were monitored by observing changes in form birefringence employing an instrumental system of our own design.

F-PM-F12 VIBRATIONAL SPECTRA OF NUCLEIC ACID. K. C. Lu, E. W. Prohofsky, and L. L. Van Zandt*; Department of Physics, Purdue University, West Lafayette, Indiana 47907

Based on a Green's function method a force constant refinement scheme is developed to be applied to the calculation of vibrational spectra of synthetic DNA molecules. These are long chain molecules with repeating units, thus the calculation using a variation of Wilson's GF matrix method can be reduced by a modified Higgs method. An initial set of force constants is chosen to calculate the frequencies then, the refinement scheme is used to fit some frequencies to experimentally observed lines by refining particular force constants. The advantage of this refining procedure in addition to its greater computational simplicity is its great flexibility. This enables one to incorporate different kinds of information into the calculation. The method can be used to internally select the force constants to be refined and to then refine to the most reasonable possible set of force constants. We have applied this method to simultaneously refine several lines in both B and A conformation DNA. We match the shifts in the frequency which occur at the conformation change. This calculation includes the motion of the ribose ring as well as other elements in the backbone.

F-PM-F13 ON THE B TO A CONFORMATION CHANGE OF THE DOUBLE HELIX. E. W. Prohofsky, and James M. Eyster,* Department of Physics, Purdue University, West Lafayette, Indiana 47907

We have investigated the B to A conformation change for poly(dG)·poly(dC) and poly(dA)·poly(dT) by a new method "soft mode analysis". In this method one examines the vibrational modes for softening i.e. frequency decreasing to zero. Such softening indicates the onset of conformational instabilities. We find theoretically that a soft mode does occur when the modes of poly(dG)·poly(dC) in B conformation are perturbed by enhanced electrostatic interactions. The enhanced electrostatic interactions mimic the effect of decreasing the polar nature of the solvent or decreasing water of hydration effects which are associated experimentally with the conformation change. A similar calculation performed on poly(dA)·poly(dT) does not cause mode softening. Both results are in agreement with experiment. The mode that softens for poly(dG)·poly(dC) gives rise to base tipping displacements which are along the direction of displacements needed to bring about the A conformation. Interactions with other vibrational modes increase the agreement between expected displacements and those required to bring about A conformation. We have also examined the effect of enhanced van der Waals interaction and these cooperate in bringing about the instability.

F-PM-F14 CONFORMATION OF ORDERED POLYNUCLEOTIDE CHAINS. W. K. Olson, Douglass College, Rutgers University, New Brunswick, NJ 08903

Empirical energy functions used previously to account for mean-square unperturbed dimensions and nmr coupling constants in randomly coiling polynucleotides have been used, after modification to estimate the conformational preferences of polynucleotide helices. Contributions to the potential energy from the interactions of atoms comprising the sugar-phosphate backbone have been separated from those involving the bases on the chain. Empirical functions have been developed to reproduce in a semiquantitative fashion both the intramolecular neighboring base stacking and the intermolecular hydrogen bonding which characterize ordered polynucleotide strands. The steric requirements of stacking and hydrogen bonding severely limit the huge population of polynucleotide helices theoretically feasible on the basis of the preferred backbone rotations. The calculations further indicate that the familiar double-stranded polynucleotide helices compromise the "ideal" stacking and hydrogen bonding geometries. Single-stranded helices found in dilute solution thus should differ significantly from the double-stranded structures characterized by X-ray studies. The effect will be most dramatic in polynucleotide chains possessing bases in an unusual high anti glycosyl conformation where the energetically preferred single-strand appears to be a left-handed helix and the favored double-strand a right-handed structure.

F-PM-F15 THE SPATIAL DISTRIBUTIONS OF RANDOMLY COILING POLYNUCLEOTIDES. R. Yevich and W. K. Olson, Douglass College, Rutgers University, New Brunswick, NJ 08903

The three dimensional spatial density distribution $W_0(\vec{r})$ of end-to-end vectors, $\vec{r}$, associated with randomly coiling polynucleotides has been determined using exact statistical mechanical methods. For long chains, the spatial distribution assumes a spherically symmetric shape which can be adequately described by a one dimensional radial distribution function, $w(R)$, where R is the magnitude of $\vec{r}$. These radial distributions agree well with the one dimensional distributions calculated from a sample of 5000 Monte Carlo chains. The values of the characteristic ratio, $\langle R^2\rangle/n\ell^2$, and the persistence vector $\langle\vec{r}\rangle$, obtained from the Monte Carlo studies agree well with those calculated from the statistical treatment described above. With shorter chains (fewer than 64 residues), however, due to constraints of fixed bond lengths, fixed bond angles, and hindered internal rotations, the shape of the spatial distribution becomes skewed and "mushroom-like". The one dimensional radial distribution only crudely approximates this more complicated form. A three dimensional representation is much more accurate and hence more useful in attempting to understand the nature of short polynucleotide segments such as those found in the single strand regions of t-RNA.

F-PM-F16 BASE STACKING IN A FLUORESCENT DINUCLEOSIDE MONOPHOSPHATE: εApεA. B.M. Baker[+*], N.R. Kallenbach, and J. Vanderkooi, Departments of Biology and Physics, Biology and Biochemistry-Biophysics, University of Pennsylvania, Philadelphia, Pa. 19174.

We have studied the optical properties of the $1,N^6$ etheno derivative of ApA, εApεA. Absorbance and CD measurements suggest the base stacking interaction in this molecule to be weaker than in ApA and that neutral salts tend to unstack it. Quantum yield measurements on εApεA prove it to be strongly quenched with respect to the monomer εAMP; in fact, this quenching increases with temperature. In the presence of 40% glycerol, however, the quenching is greatly reduced. Fluorescence lifetime measurements reveal a temperature-dependent decay which is non-linear on a semi-log plot. We have considered these data from two viewpoints: (1) two state pictures which are based on thermodynamic least squares fits to CD and quantum yield curves, together with two exponential fits to the decay curves, (2) a dynamical model in which relative motion of the two fluorophores leads to de-excitation via collision. While models of type (1) seem capable of reconciling the static properties (CD and quantum yield) it is more difficult to incorporate the dynamic properties (decay curves). Preliminary work consisting of type (2) model calculations and decay measurements in glycerol suggest this model to be most promising for detailed agreement with these experiments.

[+] C. Weizmann postdoctoral fellow.

F-PM-F17 THE ETHIDIUM BROMIDE BINDING SITE ON E. COLI $tRNA^{phe}$. Barbara D. Wells and Charles R. Cantor, Departments of Chemistry and Biological Sciences, Columbia University, New York, New York 10027.

Unfractionated E. coli tRNA and $tRNA^{phe}$ were periodate oxidized and labeled at the 3' end with dansyl hydrazine. Fluorescence titrations were performed with ethidium bromide on these tRNAs, confirming the existence of a single ethidium binding site per tRNA in each sample with a binding constant of 10^6 M^{-1}. Energy transfer between dansyl (donor) and ethidium (acceptor) was measured. Estimates of κ^2 were obtained from fluorescent polarization measurements. The distance range derived from transfer efficiencies was 29 to 40 Å. This is consistent with the NMR assignment of the ethidium binding site between base pairs 6 and 7 on the aminoacyl stem. The results with unfractionated tRNA suggest the ethidium site exists in all tRNAs. The spectral properties are consistent with intercalative binding. The tRNA binding site is 10 times stronger than the ethidium binding site on DNA. A rationale for the high affinity of this site is provided by the X-ray diffraction results which show a 2' endo ribose at residue 7. A similar sugar pucker has been observed in X-ray diffraction studies of an ethidium ribodinucleotide intercalation complex. Thus the 2'endo sugar pucker at residue 7 could predispose this area of the tRNA to intercalation.

(Supported by USPHS GM 14825-10)

F-PM-G1 RESONANT RAMAN SPECTROSCOPY OF NUCLEIC ACID COMPONENTS USING ULTRA-VIOLET LASER EXCITATION. Dan Blazej and Warner L. Peticolas, Department of Chemistry, University of Oregon, Eugene, Oregon 97403.

The first resonant Raman excitation profiles using ultraviolet radiation is presented. The compounds studied include the 5'-monophosphates of adenosine, AMP, cytidine, CMP, guanosine, GMP, and uridine monophosphate as well as the corresponding polymers and their double helical complexes. All measurements were made of dilute aqueous solutions at pH 7.0. A CMX-4 dye laser frequency doubled to the ultra-violet gave usable frequency range of 267-320 nm. In the strongly enhanced resonance region only 10^{-3} μ moles of material are needed to obtain a spectrum. The Raman bands and background due to water in the region 200 to 1700 cm^{-1} which are well-known to occur in the ordinary Raman effect do not exist in the resonance Raman effect of these materials because the water bands are not enhanced by any preresonance effect. Common salts such as NO_2^-, SO_3^{2-}, ClO_4^- which have often been used as Raman intensity standard do not exhibit any Raman bands using our UV laser radiation. However cacodylate has been shown to give a strong band at 608 cm^{-1} which can be used as an internal standard. The parameters which govern successful resonant Raman experiments using UV excitation will be discussed as well as the usefulness of this technique as a structural probe for biological macromolecules. In particular the experimental observation of the resonance Raman effect in a sample which shows strongly relaxed fluorescence will be discussed. (Supported by NIH GM 15547 and NSF GB-29709.)

F-PM-G2 MEASUREMENT OF DIFFUSION COEFFICIENT AND ELECTROPHORETIC MOBILITY WITH A QUASI-ELASTIC LIGHT SCATTERING-BAND ELECTROPHORESIS APPARATUS. T.K. Lim*, G.J. Baran*, and V.A. Bloomfield, Department of Biochemistry, University of Minnesota, St. Paul, MN 55108.

We have constructed an apparatus for the simultaneous measurement of electrophoretic mobility, μ, and diffusion coefficient, D, of macromolecules and cells. It combines band electrophoresis in a vertical, sucrose-gradient stabilized column, with quasi-elastic laser light scattering (QLS) determination of the diffusion coefficient of the species within the band. The entire electrophoresis cell is scanned through the laser beam of the QLS apparatus by a vertical translation stage. Total intensity light scattering measurement at each point in the cell gives the macromolecular concentration at that point. Solvent viscosity and electrical potential are measured at each point in the cell. Application of this apparatus to resealed red blood cell ghosts and to bovine hemoglobin indicates that measurement of field, viscosity, and migration distance are reliable, and that electroosmosis is insignificant. Application to T4D bacteriophage gives $\mu_{20,w} = (-1.05 \pm .05) \times 10^{-4}$ $cm^2/V\text{-sec}$ and $D_{20,w} = (3.35 \pm 0.10) \times 10^{-8}$ cm^2/sec for fiberless particles, and $\mu_{20,w} = -(0.59 \pm 0.03) \times 10^{-4}$ $cm^2/V\text{-sec}$ and $D_{20,w} = (2.86 \pm 0.09) \times 10^{-8}$ cm^2/sec for whole phage with 6 fibers. Phage with intermediate numbers of fibers can be detected after preparation by *in vitro* complementation. Analysis of results with the Henry electrophoresis theory for spheres indicates that each fiber contributes about 200 positive charges to the phage particle, compared with 327 from amino acid analysis. The advantages and disadvantages of this apparatus, relative to conventional electrophoresis and to electrophoretic light scattering will be discussed.

F-PM-G3 INELASTIC LIGHT SCATTERING AS A PROBE OF THE MECHANICAL PROPERTIES OF SOFT GELS. S. L. Brenner, R.A. Gelman, and R. Nossal, DCRT and NIDR, National Institutes of Health, Bethesda, Maryland 20014

Photon correlation spectroscopy is used to determine the elastic moduli of soft gels capable of sustaining long-lived mechanical oscillations. Standing displacement waves are generated in gels by random external vibrations. The dependence of observed mode frequencies on cuvette dimensions is in quantitative agreement with a simple theoretical model. Measured autocorrelation functions are found to be independent of scattering angle as predicted by theory. Elastic coefficients have been measured for agarose gels over the concentration range 0.1 to 1.0 weight percent. Results are compared with predictions of several microscopic models of entangled polymer networks. We envision that this technique can be used to study various biological materials such as cytoplasm, mucosa, and certain forms of cartilage.

F-PM-G4 PREDICTION OF ANOMOLIES IN ELECTROPHORETIC DOPPLER LIGHT SCATTERING
M.B. WEISSMAN, CHEMISTRY DEPT., HARVARD U., CAMBRIDGE, MASS. 02138

Electrophoretic light scattering reveals the mobility of concentration fluctuations,not of individual ions (1,2,3). When the Debye screening distance is much less than the scattering wavelength only fluctuations with no net charge, which cannot correspond to fluctuations in just one ionic species, are significant. Linear fluctuation theory predicts that when there are n ionic species present there are n-1 uncharged eigen-fluctuations, each with a characteristic mobility and diffusion coefficient. When diffusion is negligible one eigen-mobility occurs between each nearest pair of ionic mobilities, with one eigen-mobility being approximately zero. In general fluctuations in any one ionic concentration should travel with several different eigen-mobilities. It is in principle possible to observe more than one mobility in a solution with only one scattering species. However, fluctuations in species which contribute little to the total solution conductivity should travel only with the mobilities of those species. This theory may account for some observed anomolies in polystyrene bead scattering experiments (4).

1)M.J. Stephen (1974) J. Chem. Phys. 61 1598
2)L. Friedhoff & B.J. Berne (1976) Biopolymers 15 21
3)M.B. Weissman (1976) Dissertation, U. Cal. San Diego
4)T. Yoshimura et al. (1975) Opt. Comm. 15 277

F-PM-G5 CHARACTERIZATION OF CULTURED MAMMALIAN FIBROBLASTS BY A MULTIANGLE LIGHT-SCATTERING FLOW SYSTEM. A.M. Jamieson, A.G. Walton, Department of Macromolecular Science, Case Western Reserve University, Cleveland, Ohio; I.A. Schafer, Department of Pediatrics, Cleveland Metropolitan General Hospital, Cleveland, Ohio; B.J. Price and G.C. Salzman, Biophysics and Instrumentation Group, Los Alamos Scientific Laboratory, University of California, Los Alamos, New Mexico.

A multiangle light-scattering flow-system instrument has been used to characterize several normal cultured human fibroblast lines and abnormal lines with lysosomal storage disorders. The cells were individually passed through a focused laser beam (6328 A) at a rate of 1000 cells/sec. The scattered intensity of each cell was measured simultaneously at 32 angles between 0° and 21° with respect to the laser beam axis. After the scatter patterns were transferred to a computer, the cell types within each sample were distinguished by a mathematical clustering algorithm. In this manner, five normal skin fibroblast lines from different donors were analyzed and compared with the scatter patterns from a patient with Sandhoff's disease. In every case, there are at least two clusters present, one of which has a higher light-scattering intensity than the others over all angles. While the scattering for this cluster exhibits uniformity among the normal samples, a distinct increase in the wide-angle (> 1.6°) scattering was observed in the Sandhoff's cells. This is interpreted as being due to increased cytoplasmic turbidity from the presence of cytoplasmic inclusions due to storage of the biological material. It is found that glutaraldehyde fixation enhances the resolution between the abnormal and normal clusters at wide angles. (This work was performed under the auspices of the U.S. Energy Research and Development Administration, the National Foundation-March of Dimes, and the Cleveland Foundation.)

F-PM-G6 PYROELECTRIC EFFECT IN COLLAGENOUS MATERIALS, OBSERVED WITH PULSED 10.6 μm RADIATION. M. H. Furst,* Department of Physics and Astronomy, Hunter College, C.U.N.Y. 10021 and A. R. Liboff, Department of Physics, Oakland University, Rochester, Michigan 48063

Pulsed infrared radiation from a CO_2 laser has been used to obtain what appears to be a pyroelectric signal in a number of collagen rich substances. This technique has the great advantage over other pyroelectric methods in that sensitive a.c. detection is possible. A 250 ns pulse at 0.5 joules impinges directly on specimens of the order of 0.1 cm^2 cross sectional area and a few millimeters thick. Electric signals from different pairs of surfaces are consistently of two types, an overall polarization with a fast initial rise followed by a slower decay, as well as an oscillatory ringing. These responses appear to be, respectively, pyroelectric and piezoelectric in origin, as evidenced by similar experiments on known electrocrystalline materials such as quartz and triglycene sulfate.

F-PM-G7 COMPARISON OF COLORIMETRIC DNA DETERMINATIONS WITH FLUORESCENCE MEASUREMENTS IN THE CYTOFLUOROGRAF®. E.S. Kempner, V.H. Bono* and R.L. Dion*, NIH, Bethesda, Md. 20014

Determining the distribution of DNA content in individual cells of a population has been made feasible by the development of flow techniques to measure the fluorescence of large numbers of individual cells containing DNA-bound stains. Within a single experiment, relative changes of DNA content can be easily detected. To widen the usefulness of the techniques, it is necessary to be able to compare results of different fluorescent stains, to understand the effects of different fixatives and other details of technique, and to establish absolute values of cellular DNA concentration. The average DNA of murine leukemia (L-1210) and Euglena gracilis cells from control and mitotically-inhibited cultures were measured by standard colorimetric techniques (diphenylamine and indole reactions). The DNA content of individual cells was measured in the Cytofluorograf® with both Feulgen-stained and propidium iodide-stained cells. Various parameters such as fixation and staining techniques were optimized. Computer analysis of the spectra (DNA/cell) yielded the mean DNA per cell. Changes in average cellular DNA between control and drug-inhibited cells were compared among the four methods. Although all were qualitatively similar, best agreement was obtained between colorimetric measurements and propidium iodide staining. Analysis of the spectra revealed shifts in staining efficiency due to inhibitors. Quantitative relationships between the DNA content of G_1 and G_2 phase cells varied from ideal due to several experimental factors (endoreduplication, non-linearity of staining, doublet particles).

F-PM-G8 MEASUREMENT ACCURACY IN ANALYTICAL PARTICLE ELECTROPHORESIS (APE): EVALUATION OF POTENTIAL SOURCES OF ERROR. F.J. Nordt, R.J. Knox and G.V.F. Seaman, Department of Neurology, University of Oregon Health Sciences Center, Portland, Oregon 97201.

APE is used in many biological applications including characterization of cell surface structure, determination of the probable success of electrophoretic separation of subpopulations of cells and in diagnosis of certain diseases. These applications require collection of accurate data. However, a survey of the literature indicates that erroneous data are reported due to oversights of potential sources of error inherent in equipment design and operation. These sources include fluid flow contributions to the measured particle velocity (electroosmosis (u_o) and thermal convections), ill-defined voltage gradient (electrode polarization, localized thermal gradients) and errors in particle velocity measurements (timing, calibration of the graticule, optical effects). Optimization of design features and suitable operation conditions requires evaluation of these factors. Remedial measures for many of the problems are in principle available including the use of low zeta potential surface coatings to eliminate u_o, the use of open APE chambers with geometries selected to minimize certain types of convective flow and the use of a constant current mode to eliminate voltage gradient fluctuations. However, the nature of the interactions of these factors has not been established so that remedial measures aimed at elimination of a particular factor such as u_o may enhance other problems. It is therefore imperative to optimize chamber design from the standpoint of fluid dynamics and establish the nature of the critical design variables and the magnitudes of relevant chamber parameters and operation variables. From such an analysis optimal combinations of remedial measures can be designed in order to minimize measurement errors. Supported by the National Institutes of Health, Research Grant HL 18284 and NASA Contract NAS8-32162.

F-PM-G9 NEW TEMPERATURE JUMP METHOD FOR HETEROGENEOUS SYSTEMS. G. H. Czerlinski, Department of Biochemistry, Northwestern University, Chicago, Ill. 60611

A temperature jump method was developed and tested which utilises the absorption of magnetic energy by specially selected mediators for heating. The apparatus produces temperature jumps through coupling of pulsed magnetic fields (damped oscillations) to selected particulate mediators in aqueous suspensions. Two substances were tested representing two different types of mediators. "Direct" coupling produced a temperature rise of o.3°C, "indirect" coupling one of o.2°C. Both changes were measured by special alcohol thermometer after ten pulses at maximum field strength (both water and methanol were used as controls). Suitable modification of mediators should lead to temperature rises which are at least ten times the above value for "direct" coupling and at least 100 the above value for "indirect" coupling (same design). As ordinary biological objects provide no hindrance to the penetration of magnetic fields, properly distributed mediators could produce well differentiated and localized heating in living organisms. This basic method depends upon several parameters which permit a multitude of different applications in biology and possibly medicine. In the latter case, highly selective "differential hyperthermia" is envisioned. (The experimental part was supported by a grant from the National Science Foundation to the Medical Foundation of Buffalo.)

F-PM-G10 AN IMPROVED METHOD FOR STUDYING THE PHYSICAL CHEMISTRY OF BUBBLE FORMATION. Joseph S. D'Arrigo. Physiol. Dept., U. of Hawaii School of Medicine, Honolulu, HI 96822.

Over the last decade, bubble formation in gelatin has provided an extremely useful model for studying the etiology of decompression sickness in humans. From these and other studies, it has become clear that bubbles originate in water and probably also in humans as pre-existing gas cavitation nuclei, which must be held intact by surface-active "skins" that are gas-permeable (Yount, Kunkle, D'Arrigo, Ingle, Yeung & Beckman (1976) Aviation, Space & Environ. Med. (In press)). In order to further study the physical properties of the surfactant "skins" surrounding gas cavitation nuclei, a different gel method was developed which utilizes agarose as the gelling substance. Unlike gelatin, agarose is an uncharged, relatively inert, homogeneous polysaccharide that is commercially available in highly purified form. Contrary to the results from experiments using mammalian gelatin, it was found that saturation (for 16 hours) of agarose gels with either CO_2, N_2, or He yield cavitation thresholds which are approximately equal and lower than those obtained with gelatin. In particular, one CO_2 bubble cound be produced in a 0.27 ml agarose sample (in 50% of trials) by a rapid decompression of only -3.2 psig ($\approx$ -1/5 atm). These and other data lead to the conclusion that while the type and amount of dissolved gas surrounding a bubble is important for its growth and persistence, these factors are not important for its initial formation from a gas cavitation nucleus upon rapid decompression. It is suggested that the transformation of a stable gas nucleus into an unstable bubble, upon rapid decompression, results primarily from an expansion of the gas already trapped within the gas cavitation nucleus following the saturation period. With a suprathreshold decompression, this expansion of gas within the nucleus must "burst" the surfactant "skin" surrounding and stabilizing the gas cavitation nucleus. (Grant Sup: NSF No. BNS76-02647, NOAA No. R/DP-02)

F-PM-G11 THE KIRLIAN PHANTOM LEAF PHENOMENON. Y.T. Thathachari and S.Pushpa*, Indian Instt. of Technology, Madras, India and University of California, San Francisco, CA 94143.

In Kirlian photography the object to be imaged is placed in a high voltage high frequency electric field which is the only source of illumination. The images which bear enough resemblance to the object for recognition are characterized by many luminous spots or streaks. Terms like aura, energy body or bioplasma are freely used in the Kirlian literature to describe the distribution of these spots and the changes induced in them. There is no compelling necessity, as yet, to invoke either these terms or the concepts that accompany them. In a systematic study, we carried out over 1500 carefully planned experiments using objects of various shapes, texture and composition. The objects and the recording emulsions were placed in lightproof casettes in the electric field provided by a Tesla coil. Multiple films and screens were also used at times on either side of the objects. The thickness and to some extent, the shape of the airgap could be controlled. We imaged metal coins, their collodion replicas, composites with a planned structured distribution of materials and presenting smooth surfaces, leaves of various shapes and texture subjected to physical and chemical treatments, millipedes and cockroaches. Our Kirlian pictures were sharper and more detailed than many that have been so far published. We recorded, under truly acceptable conditions, the picture of a cut leaf in which the image of the missing portions was clearly reproduced. The boundary was visible; but the details in the intact and cut portions were different. We still feel there is no need yet to invoke bioplasma to explain the phenomenon. It is not unlikely that the shape of the airgap in the region of the cut away portion of the leaf and emissions from the boundary may contribute to the effect. However, this does not explain all the details.

F-PM-G12 A FLUORINE-19 NMR RELAXATION STUDY OF GALACTOSE OXIDASE. B. J. Marwedel,* R. J. Kurland, The Bioinorganic Group, Departments of Chemistry and Biochemistry, SUNY at Buffalo, Buffalo, N. Y. 14214.

Fluoride ion has not been used extensively as a NMR relaxation probe of paramagnetic metalloproteins, possibly due to the unusual sensitivity of fluoride ion relaxation rates to relatively slight changes in ionic strength, pH, temperature, and paramagnetic impurities. However, the sensitivity of F^- relaxation rates to paramagnetic effects can be an asset in the study of metalloproteins: paramagnetic relaxation rate enhancements observed for fluoride ion are usually much greater than those for water protons. Detailed relaxation rate measurements using F^- and water protons as probes of the Cu^{+2} containing enzyme galactose oxidase (E.C. 1.1.3.9), are reported. Competition experiments with CN^- show that 85-90% of enzyme-bound F^- is bound to or near the Cu^{+2} center. Similar experiments with the substrates galactose and dihydroxyacetone demonstrate that the Cu^{+2} ion is at or very near to the active site of the enzyme. Relaxation rate data at high galactose concentrations suggest that a conformational change of the enzyme-substrate system may occur. Results of variable temperature and frequency measurements imply that the relaxation mechanism is modulated by an exchange correlation time. Kinetic experiments involving the $Fe(CN)_6^{3-}$, $Fe(CN)_6^{4-}$ couple indicate that the binding sites for the two complexes are not the same, in agreement with other data obtained within our group.

Support from the National Science Foundation is gratefully acknowledged.

F-PM-G13 THE NMR DETECTION OF MALIGNANCY IN SPECIMENS OF HUMAN TISSUE. M. Goldsmith, J. Koutcher*, R. Damadian, Department of Medicine & Program in Biophysics, Downstate Medical Center, Brooklyn, New York 11203

Over eight hundred (800) specimens of human tissue taken from six hundred and fifty (650) individuals, were inspected by proton magnetic resonance techniques (at 22.5 Megahertz). The purpose of the study was to evaluate the diagnostic capabilities of the nuclear magnetic resonance (NMR) technique with regard to the detection of malignancy. The combination of two NMR parameters (spin-lattice (T_1) and spin-spin (T_2) relaxation times) into a malignancy index yielded excellent discrimination between the two populations of tissue. In gastro-intestinal tissue for example, the mean and standard deviations obtained were 2.004 ± 0.342 for normal tissue, and 3.266 ± 0.642 for malignant specimens. In addition, the NMR technique indicated that histologically normal tissue taken adjacent to the malignancy was pathologically "involved". Analysis of the electrolyte and water content of such tissues confirmed this abnormality.

F-PM-G14 WATER PROTON MAGNETIC RESONANCE OF METABOLIC AND AMETABOLIC ARTEMIA EMBRYOS. P.K. Seitz*, J.S. Clegg* and C.F. Hazlewood, Dept. of Pediatrics, Baylor College of Medicine, Houston, Tx 77030 and Dept. of Biology, University of Miami, Fl 33124.

Pulsed nuclear magnetic resonance (NMR) has been used to study the motional freedom of water during the onset of metabolism in embryos of the brine shrimp, Artemia salina. The Artemia gastrula occurs naturally in a highly dessicated, encysted state. Water absorbed through the cyst shell triggers re-initiation of metabolism. The level of hydration apparently regulates the nature and extent of the metabolic reactions which take place. T_1 and T_2 relaxation times of water protons in the cysts have been measured over a wide range of hydration levels. Results indicate that T_1 and T_2 are not simple monotonic functions of water content. There exist minima in the T_1 and T_2 values at approximately 30g H_2O/100g dried cysts. Multicomponent analysis of the relaxation data reveal at least two distinct fractions of water not in rapid exchange. The slower relaxing T_2 fraction exhibits a different pattern with respect to hydration than do the initial T_1 and T_2 relaxation rates. The self-diffusion coefficient of water in the cysts has also been measured and shows a tenfold decrease (compared to pure water) for even the most highly hydrated cysts. D in the less hydrated samples is even lower, 10^{-7} cm^2/sec. Supported by: R.A. Welch Foundation, GM-20154, R.R-0188, NSF GB-40199, and ONR N0014-75-A-0017.

F-PM-G15 USE OF LASER DYES AS FLUOROCHROMES. D. Gill, Physics Department, Ben-Gurion University of the Negev, Beer Sheva, Israel.

Fluorochrome stains, used in fluorescence microscopy, share with laser dyes the specifications of efficient fluorescence and low rate of fading. Fluorochroming can benefit from laser-dye technology in adopting the methods of quantitative organic luminescence. Cresyl violet is brought as an example.